JOSHUA

The Journal of Science and Health at the University of Alabama

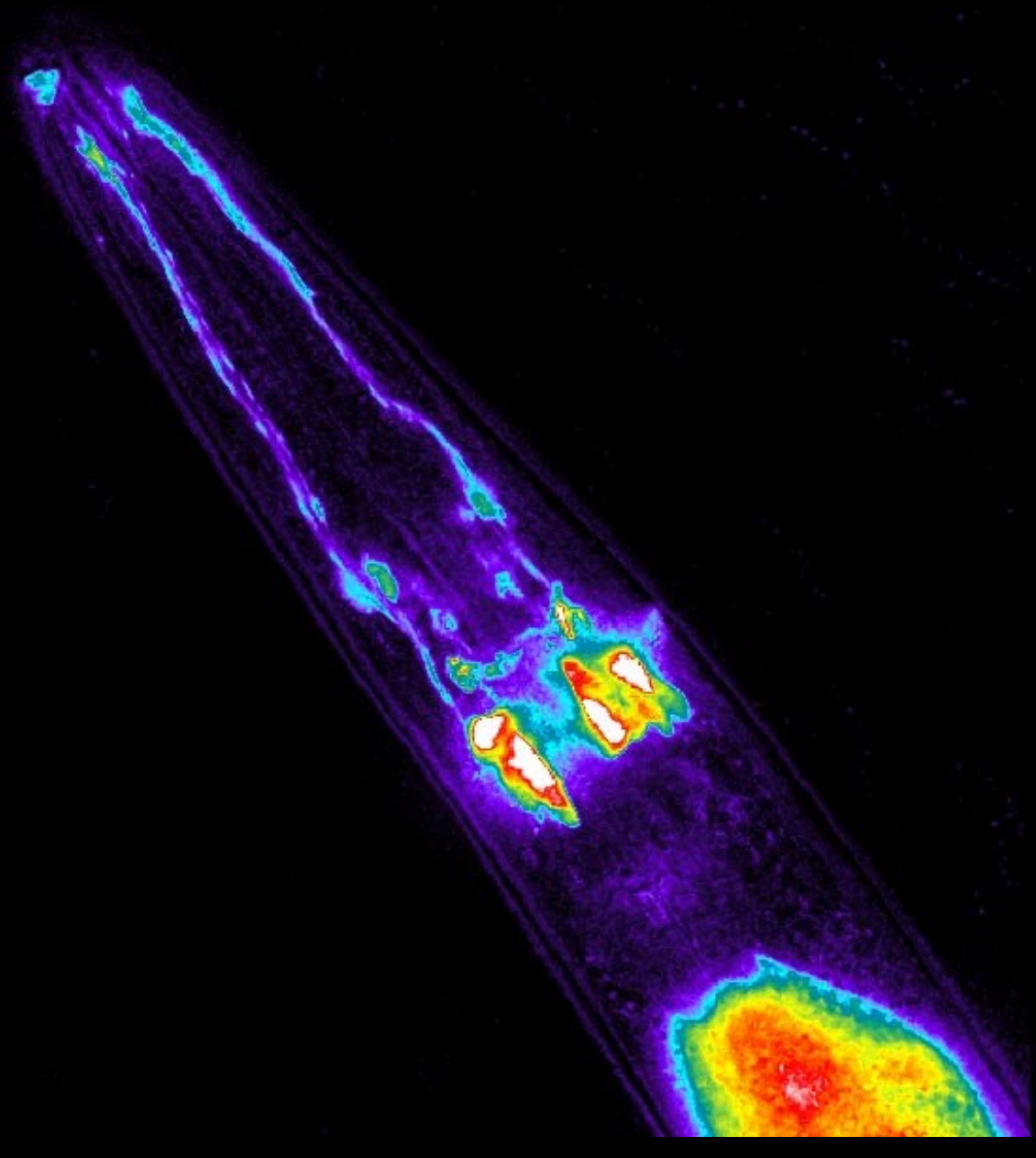

2016 **Volume 13**

About the Cover:

Caenorhabditis elegans, commonly known as C. elegans is a free-living nematode. This hermaphroditic pseudocoelomate has been used as a model organism for research into neuronal development due to its simplistic nervous system and transparency. This picture was taken by the Caldwell Lab, alternatively known as the Worm Shack., at the University of Alabama.

2015-2016 JOSHUA Staff

Questions should be directed to joshua.alabama@gmail.com, and more information and all archived volumes are available at bama.ua.edu/~JOSHUA.

Table of Contents

Characterization of IgGI Antibodies Expressed in CHO Cells by ELISA and RP-HPLC
Joanna Urli ……..……..……...……..……..…...**4**
.
Magnetic Nanoparticles for Use in Magnetically Triggered Drug Release for Cancer Therapy
Kaylee O'Connor ..……..……..…...…..**8**

Synthesis of α-FeOOH and CoP_i Thin Films for use as Catalysts in Electrochemical Water Oxidation and Efficiency Comparison to Known Effective Catalysts
Jeremy Hitt…. ……...……..…….**12**

Construction and Characterization of p-type heterojunction CuO|$CuBi_2O_4$ photocathode electrode for photoelectrochemical reduction of water as sustainable source of energy
Kieran Bhattacharya ……..…..……..**17**

Utilization of Corn Cob by Clostridium tyrobutyricum and Clostridium cellulovorans and Characterization of the Inhibition Factors
Matthew Pate…..……..…….**22**

Exploring HIV Stigma in the US Virgin Islands
Elizabeth Di Valerio…….……..…….**27**

Evolutionary Optimization of Aircraft Landing Gears
Robert Ramsey…..…….…….....…....…...…….**32**

Mechanisms of Ethanol-Induced Developmental Neurotoxicity
Courtney Rentas……..…….....……..**37**

A Study of the Role of Music and Religion on African American Adolescent Females' Sexual Beliefs and Behaviors
Makenzie Plyman ……..…….....…..**43**

Interview with Richard Myers
JOSHUA…….……..…..**48**

Characterization of IgG1 Antibodies Expressed in CHO Cells by ELISA and RP-HPLC

Joanna Urli[1], Theresa Borcky[1], Kelley Cooper[1], Joseph James[1], Kyle Leonard[1], Justine Panian[1], Marybeth Taglieri[1], Ningning Xu*1*, and Margaret Liu[1]

Faculty Mentor: Margaret Liu

[1]*Department of Chemical and Biological Engineering, The University of Alabama, Tuscaloosa, Alabama 35487*

Enzyme-linked immunosorbent assay (ELISA) and high performance liquid chromatography (HPLC) are two of the most widely used analytical tools to quantitate recombinant monoclonal antibodies. In this study, both an ELISA method and a HPLC method were developed for monitoring and characterizing the production of intact IgG1 antibodies in CHO cell culture supernatant. The sensitive sandwich ELISA assay was comprised by a goat anti-human IgG H&L antibody and a peroxidase labeled anti-human IgG H&L antibody. In addition, the RP-HPLC method was developed based on an octylsilane HPLC column (Viva C8) incorporated with high column temperature (70°C), two organic solvents (acetonitrile) containing 0.08% trifluoroacetic acid (TFA), and flow rate of 0.5 mL/min under a gradient elution condition. These two methods are being used to efficiently evaluate antibody productions during CHO producing cell line development.

Introduction

Monoclonal antibodies (mAbs) are large glycoproteins that consist of two identical heavy chains and two identical light chains connected by covalent disulfide bonds. Immunoglobulin G, the most common type of antibody, has become an important therapeutic modality, growing a large class of biologics to treat multiple human diseases and particular cancers. IgG antibodies have been engineered to specifically bind ligands on certain cancer cells, leading the immune system to recognize these cancer cells and destroy them via triggering antibody-dependent cellular cytotoxicity (ADCC) and/or complement-dependent cytotoxicity (CDC) [8]. The majority of recombinant mAbs that are genetically engineered for mammalian cells are able to be expressed in Chinese hamster ovary cells (CHO), as CHO cells offer proper folding and efficient post-translational modification on recombinant proteins that can increase the efficacy of protein therapeutics [5,6]. During the cell line development, the recombinant IgG1 are monitored to evaluate the productivity of cells and to identify high producer clones.

Enzyme-linked immunosorbent assay (ELISA) is a widely used biochemical method to rapidly detect proteins with advantages of high specificity and high sensitivity [1]. Although ELISA has been developed to analyze different proteins, the principles are the same. The antigen or first antibody coats the solid surface of micro-well plates, then the specific proteins interact with the antigen or first antibody, while others are washed away during the assay, next the secondary enzyme-conjugated antibody and substrate are used to create a measurable signal [3]. ELISA is very helpful in rapid screening of a large number of samples and accurately quantitating specific proteins even in low concentrations.

High-performance liquid chromatography (HPLC) is a process by which mAbs and other protein molecules can be separated from a solution of cells based on their polarity. The column is the most pivotal factor in developing HPLC method. HPLC methods with the use of ion exchange columns or size exclusion columns have been well-developed tools for quantitating intact antibodies. Reversed phase (RP) HPLC is becoming a promising approach to analyze intact antibodies, due to the new generation of wide pore RP stationary phases. The reversed phase method separates samples based on the differences in hydrophobicity, when the solute protein molecules inside the mobile phase are bound to the immobilized hydrophobic ligands on the stationary phase [2]. RP-HPLC is considered a powerful tool in analyzing proteins, due to its versatility in analyzing a wide variety of samples with high resolution via easily adjustable mobile phase conditions [4]. In this study, the ELISA method was utilized for quantitating the recombinant IgG1 productions in CHO cell culture with low concentration, or in the limiting cloning steps where thousands of wells containing cultures from single cells are screened to select high producing clones; while the

RP-HPLC method was utilized for titrating the recombinant IgG1 productions expressed in CHO cells with high concentration.

Materials and Methods

Recombinant IgG1 from CHO Cell Culture

Both CHO DG44/IgG1 and CHO K1/IgG1 stable cell lines were developed for recombinant IgG1, using the lipid based transfection, followed by selection, amplification, and cloning [7]. The CHO DG44/IgG1 cells were cultivated in CD optiCHO medium with 8 mM L-glutamine in shaker flasks. CHO K1/IgG1 cells were maintained in CDM4CHO medium in shaker flasks. These cells were incubated in a CO_2 incubator at 37°C with an orbital shaker rotating at 120 rpm. The CHO cell cultures with recombinant IgG1 were collected and centrifuged, and then the supernatants were taken out and stored at -80°C for ELISA and/or RP-HPLC assays.

Antibody Quantification by ELISA

Nunc-Immuno™ MicroWell™ 96-Well Plates (Thermo Scientific) were coated with goat anti-human IgG H&L (2ug/mL, Abcam) in 50 mM carbonate-bicarbonate buffer (pH 9.6) at 4°C overnight. The plates were then blocked by 2% BSA at 4°C overnight. Serial dilution of IgG standard (Jackson-immunoResearch) or cell culture supernatant samples were added into wells of coated plates and incubated at 37°C for 1 hour. The peroxidase-labeled anti-human IgG (H&L) (50 ng/mL, KPL) was then added into the wells as the detected antibody and incubated at 37°C for 30 minutes. Each incubation step was followed by wash using PBS buffer with 0.05% Tween 20. 1-Step™ Ultra TMB (Thermo Scientific) was added as a substrate and incubated at room temperature for 30 min. The reaction was stopped by 1M H_2SO_4, and the optical absorbance was tested at 450 nm with a plate reader.

Antibody Quantification by RP-HPLC

RP-HPLC was executed on Shimadzu LC-20A HPLC system that consisted of an auto-sampler, two pumps, a column oven, a UV detector, and a controller. Various oven temperatures (25°C, 50°C, 60°C, 70°C, and 80°C), flow rates (0.2 mL/min and 0.5 mL/min), and UV wavelengths (215 nm, 254 nm, and 280 nm) were tested during method development. The optimal method employed Viva C8 column (2.1mm×100 mm, 5 um particle size, 300 Å pore size), temperature of 70°C, flow rate of 0.5 mL/min, and UV 215 nm. The mobile phase A was 10% acetonitrile with 0.08%TFA, while the mobile phase B was 90% acetonitrile with 0.08%TFA. The gradient programs started at 0% of solvent B, and held for 5 min. It was then increased to 60% of solvent B in 10 min, and kept at 60% for 5 min. Subsequently it was decreased to 0% of solvent B in 0.1 min, and held for 2 min.

Results and Discussion

ELISA Method Development

The primary antibody and the secondary antibody are very important factors in the development and the optimization of ELISA method. In this study, serial concentrations of primary antibody and secondary antibody were tested to determine their optimal concentration. The 2 ug/mL of goat anti-human IgG H&L and 50 ng/mL of peroxidase-labeled anti-human IgG (H&L) were chosen with the increased signal-to-noise ratio. A dilution series of IgG1 standard proteins, from 0 ng/mL to 250 ng/mL, were measured to establish the calibration curve that had a R-squared value of 0.99992. When analyzing the unknown samples, several dilutions were also performed, and the standard curve was required to be run each time of analysis.

RP-HPLC Method Development

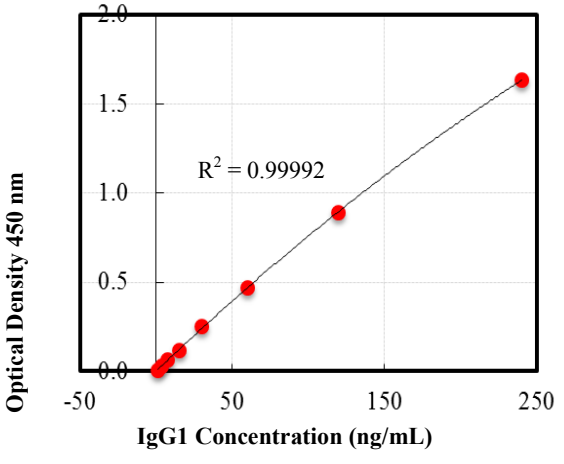

Figure 1. Calibration curve constructed for IgG1 quantitative analysis by ELISA

Viva C8 column (2.1mm×100 mm, 5 um particle size, 300 Å pore size) was used to screen and optimize ideal separation parameters for intact IgG1 separation. Different oven temperatures (25°C, 50°C, 60°C, 70°C, and 80°C) were tested, and the results showed that peak tailing and broadening were significantly reduced when the temperature was increased. However,

an excessively high temperature might cause thermal degradation of antibodies and shorten the life of column. Therefore, the temperature of 70°C was applied in this RP-HPLC method. The use of an ion-pairing agent TFA in mobile phase could also suppress peak tailing and broadening. Flow rates of both 0.2 mL/min and 0.5 mL/min were evaluated, and the results showed that the faster flow rate (0.5 mL/min) generated better peak shape and deceased the analysis time. In addition, different UV wavelengths (215 nm, 254 nm, and 280 nm) were also tested and finally the UV 215 nm was selected due to its stable baseline. After the RP-HPLC method was developed and optimized, the IgG1 protein standards with different concentrations were analyzed to create the calibration curve shown in Figure 2. The range of IgG1 concentrations was from 0 ug/mL to 200 ug/mL, correspondingly the peak areas of IgG1 proteins were from 0 to 9,766,192. The line obtained had a R-squared value of 0.99996, which was used to calculate IgG1 concentrations in cell culture supernatant samples.

Characterization of Recombinant Antibodies from CHO Cell Culture

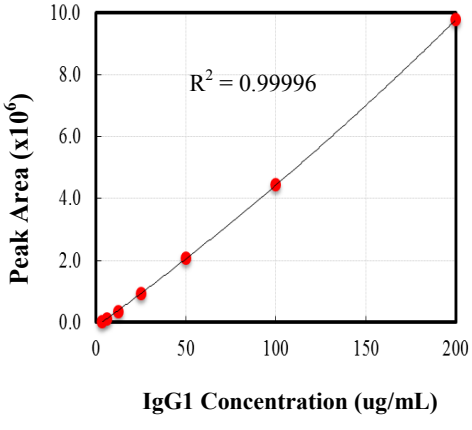

Figure 2. Calibration curve constructed for IgG1 quantitative analysis by RP-HPLC

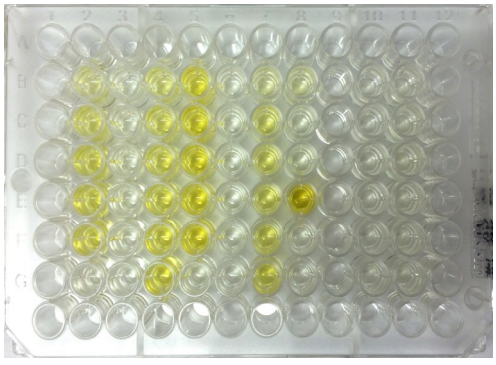

Figure 3. Representative photo of IgG1 protein in ELISA

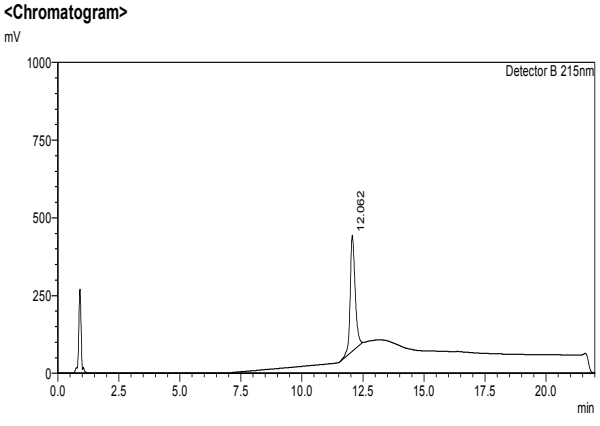

Figure 4. Representative chromatograms of IgG1 protein

Samples were collected from the culture CHO antibody producing cell lines, and the concentrations of recombinant IgG1 were analyzed using both ELISA and HPLC methods as a comparison test. One of these samples was subjected to 1/1000 dilution and tested using ELISA shown in Figure 3, and the calculated concentration was 103.5 ug/mL. Correspondingly, the IgG1 concentration in these samples, obtained by HPLC assay, was 105.2 ug/mL, and the chromatography is shown in Figure 4. The results confirmed that the developed ELISA and HPLC methods were valid to characterize the recombinant IgG1 antibodies in CHO cell cultures.

Conclusion

The sensitive sandwich ELISA method and efficient RP-HPLC method were successfully developed and optimized to quantitate the intact IgG1 anti-

bodies expressed in CHO cells. This work represented one of the typical analytical methods for mAbs characterization, which facilitated the development of CHO antibody producing cell line.

References

[1] Dixit CK, Vashist SK, O'Neill FT, O'Reilly B, MacCraith BD & O'Kennedy R. (2010). Development of a high sensitivity rapid sandwich ELISA procedure and its comparison with the conventional approach. Anal. Chem, 82(16): 7049-7052.

[2] Fekete S, Veuthey JL, Eeltink S & Guillarme D. (2013). Comparative study of recent wide-pore materials of different stationary phase morphology, applied for the reversed-phase analysis of recombinant monoclonal antibodies. Anal. Bioanal. Chem, 405(10): 3137-3151.

[3] Kai J, Puntambekar A, Santiago N, Lee SH, Sehy DW, Moore V, Han J & Ahn CH. (2012). A novel microfluidic microplate as the next generation assay platform for enzyme linked immunoassays (ELISA). Lab Chip, 12(21): 4257-4262.

[4] Staub A, Guillarme D, Schappler J, Veuthey JL & Rudaz S. (2011). Intact protein analysis in the biopharmaceutical field. J. Pharm. Biomed. Anal, 55(4): 810-822.

[5]Urli J, Panian J, Facchine E, Steadman M, Brankston B, Borcky T, Xu N & Liu M. (2015) High Productivity, Serum-free, Suspension CHO Cell Culture Process Development for Anticancer Therapeutic Protein. JOSHUA, 35.

[6] Xu N, Ma C, Sun W, Wu Y & Liu XM. (2015). Achievements and perspectives in Chinese hamster ovary host cell engineering. Pharmaceutical Bioprocessing, 3(4): 285-292.

[7] Xu N, Ou J, Gilani AKA, Zhou L & Liu M. (2015). High-level expression of recombinant IgG1 by CHO K1 platform. Frontiers of Chemical Science and Engineering, 9(3):376-380.

[8] Zhou L, Xu N, Sun Y & Liu XM. (2014). Targeted biopharmaceuticals for cancer treatment. Cancer let., 352(2):145-151.

Acknowledgements

This work was supported by the Research Grant Committee (RGC), a grant from the Department of Chemical and Biological Engineering, and funding by the National Science Foundation (BRIGE 24512). Furthermore, we would like to thank our parents for always encouraging us to strive to do our best.

About the Author

Originally from Massapequa, New York, Joanna Urli is a junior studying Biology at The University of Alabama. She has been working in Dr. Margaret Liu's lab for two and a half years. She presented her research at the AIChE National Conference in Atlanta, Georgia in November 2014, at the AIChE Southern Regional Conference in Tuscaloosa, Alabama in March 2016, and at the National Conference on Undergraduate Research in Asheville, North Carolina in April 2016. She would like to thank Dr. Liu and Ningning Xu for their patience and support.

Theresa Borcky is a junior from Germantown, TN, majoring in Biology at the University of Alabama. She has been a part of Dr. Margaret Liu's lab for two years, and presented on behalf of her lab at the University of Alabama Undergraduate Research Conference in 2015. She appreciates Ningning Xu and Dr. Liu for all they have taught her over the past two years.

Magnetic Nanoparticles for Use in Magnetically Triggered Drug release for Cancer Therapy

Abigail L. Paulson, Kaylee M. O'Connor, and David E. Nikles

Faculty Mentor: David E. Nikles

Department of Electrical and Computer Engineering, The University of Alabama, Tuscaloosa, AL 35487

The purpose of this project is to synthesize magnetic nanoparticles to be used in a system that delivers chemotherapy drugs to cancer cells without impacting the rest of the cells in the body. Single crystal magnetite nanoparticles of varying sizes were synthesized by the thermal decomposition of iron oleate in high boiling organic solvents (benzyl ether or 1-octadecene). X-ray diffraction and high-resolution X-ray photoelectron spectra were used to characterize the particles by diameter and size distribution. The effects of varying reaction time and temperature on the properties of the nanoparticles were studied in order to determine the optimal synthesis procedure..

Introduction

Cancer is one of the leading causes of death worldwide, accounting for nearly one in four deaths in the United States. Approximately 39.6% of men and women in the United States will be diagnosed with cancer at some point in their lives, and an estimated 595,690 deaths will occur due to cancer in 2016 [2]. The current treatments for cancer include radiation, surgery, chemotherapy, hormone therapy, and immunotherapy.

Chemotherapy involves infusing toxic drugs into the body, which kills both healthy somatic and cancerous cells. In order to minimize these harmful side effects, a more effective way of delivering chemotherapy drugs to cancerous sites needs to be developed. The goal of this project is to develop a targeted, magnetically triggered drug delivery system which will release drugs at specifically targeted cancerous cells. The method is to synthesize magnetic nanoparticles and modify the surface chemistry of these particles. The addition of targeting and drug-release ligands will allow the drug delivery to be location specific, since the targeting will direct the delivery system to the cancer site. We propose the use of magnetic induction heating to allow the release of the drug from the system at the targeted location. The specific paramagnetic properties of magnetite nanoparticles allows them to heat by magnetic induction. In the proposed system, this magnetic induction heating will trigger the release of drugs.

The specific absorption ratio (SAR) is a measure of the amount of heat generated during magnetic induction measured in watts per gram of particle. Our objective is to make particles with the highest value of SAR. Nanoparticles must be small enough to maintain their superparamagnetic properties, but must be large enough to heat efficiently, shown by large SAR values. It is important to have a narrow particle size distribution since the magnetic properties of particles in the nanoscale regime vary greatly with size. If there is a broad particle size distribution, particles at the low end will have vastly different properties than particles at the high end of the distribution. This has motivated the current study to develop particle chemistry to control size and distribution of particle sizes.

A variety of literature methods are available for the synthesis of magnetite nanoparticles, although they vary in the yield, scalability, and reaction difficulty [2,3,5,6]. The Hyeon method [3] was chosen for this project because of the availability and relative simplicity of the reaction. According to these papers, the size and composition of the iron oxide nanoparticles can be fine tuned by modifying the reaction solvent and reaction time. Optimizing the properties of the magnetic nanoparticles will allow for more effective heating and drug release.

Particle Synthesis

As mentioned above, the Hyeon method was used to synthesize magnetic nanoparticles through the high temperature decomposition of iron II oleate. We varied reaction times and reflux temperatures in order to determine the effect on particle size and particle distribution.

The specific methods used in the synthesis of the iron oxide nanoparticles described in this paper are listed below.

Iron Oleate Complex

The iron oleate complex was prepared by dissolving 10.8 g iron (III) chloride and 36.3 g sodium oleate in a mixture of 80 mL ethanol, 60 mL distilled water, and 140 mL hexane in a 500 mL round-bottom flask fitted with a reflux condenser. The mixture was heated for four hours in an oil bath at 70 ˚C with magnetic stirring under a nitrogen atmosphere. The reaction was allowed to cool, then transferred to a separatory funnel. The solution was washed with 50 mL of distilled water five times, and then the hexane solution was dried with an excess of magnesium sulfate. The solution was filtered via vacuum filtration and transferred to a crystallization disk. The dish was placed in the vacuum to evaporate the hexane. The vacuum oven was heated to 60 ˚C to further dry the iron Oleate.

Iron oxide nanoparticles.

Nanoparticles are synthesized by thermal decomposition of iron oleate in the presence of oleic acid with either 1-octadecene or benzyl ether. A 1000 mL three-neck round bottom flask was equipped with a thermometer and thermometer adaptor, reflux condenser, magnetic stirring, nitrogen atmosphere, and a heating mantle. 36g iron oleate, 200 g of solvent (either 1-octadecene or benzyl ether), and 5.62 g oleic acid were added to the flask. The reaction mixture was heated to reflux and the heating time varied as shown in Table 1. The solution was allowed to cool, and 500 mL ethanol was added to the reaction mixture as it stirred in order to precipitate the particles.

The reaction mixture was transferred to a 1000 mL Erlenmyer flask and placed on a neodymium iron boron magnet, which pulled the particles out of solution. The reaction solvent then was decanted off. The reaction mixture was first shaken with 300 mL acetone, and placed on the magnet overnight to precipitate the particles. The particles could be seen at the bottom of the flask, and excess acetone was decanted away. Next, an adequate amount of hexane was added to redisperse the particles into solution. 250 mL of acetone was then added and the process repeated. As cleaning progresses, ethanol should be used instead of acetone to avoid stripping the oleic acid off of the surface of the particles. Cleaning solvent amounts can be decreased from 300mL as the process continues.

Results

Two reaction solvents were used in the thermal decomposition reaction. The Hyeon method states using 1-octadecene. However, previous work in our lab has shown that 1-octadecene is very hard to remove from the resulting reaction mixture. In order to avoid this problem, benzyl ether was used instead of 1 -octadecene. The Hyeon method also suggests cleaning the mixture using 500 mL ethanol and centrifugation. However, centrifugation was time consuming, difficult, and produced a very small yield. Using the strong permanent magnet, particles can be pulled out of solution leaving behind impurities. This provides a more efficient method of cleaning particles. We found acetone was very efficient in cleaning particles, however it stripped off oleic acid ligands. The particles could no longer be dispersed in hexane, and oleic acid was added drop by drop to cause the particles to disperse when this problem occurred.

The reaction time was varied for the thermal decomposition reaction, from the literature specified 30 minutes, to a maximum of 75 minutes. This increase was done in increments of 15 minutes in order to determine the fine effects that reaction time has on the nanoparticle size and size distribution.

X-ray diffraction (XRD) was used to determine the unit cell size of the magnetite particles. Fig. 1 shows the XRD curve for sample AP013. This curve was typical of the XRD curve obtained for iron oxide particles from different reactions. The diffraction peaks in Fig. 1 were indexed to the known diffraction peaks for magnetite and were consistent with a cubic structure having a unit cell size of 836.9 ± 0.9 pm.

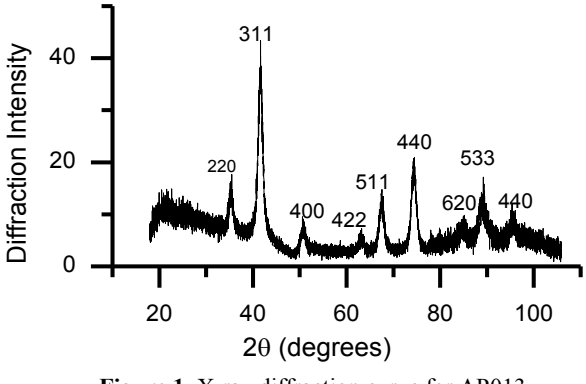

Figure 1. X-ray diffraction curve for AP013.

Although the X-ray diffraction curves for the iron oxide nanoparticles were consistent with magnetite, it was difficult to distinguish between magnetite and maghemite phases by X-ray diffraction since the unit cell parameters and lattice types are similar [1]. X-ray photoelectron spectra can be used to distinguish between Fe_3O_4 and gamma Fe_2O_3 [7]. The X-ray photoelectron spectra in the Fe 2p binding energy region shows two peaks due for commercial maghemite (Fig. 2a). This was due to due to spin-orbital splitting of the energies for the Fe 2p orbitals, giving a low energy peak 2p and a high energy peak, 2p. The XPS curve also had satellite peaks indicative of maghemite phase. These satellite peaks were also seen in the spectrum for AP003 (Fig. 1b) and AP013 (Fig 2b). Hyeon and coworkers have prepared a series of iron oxide nanoparticles having different diameters by the thermal decomposition of iron(III) oleate. X-ray absorption edge spectra and X-ray magnetic circular dichroism spectra showed that the phase composition $(\gamma\text{-}Fe_2O_3)1\text{-}x(Fe_3O_4)x$ varied with increasing particle diameter from maghemite for 5 nm particles to magnetite for 22 nm particles. The observation from the XPS that the 7 nm diameter particles were maghemite is consistent with the results reported by Hyeon and coworkers.

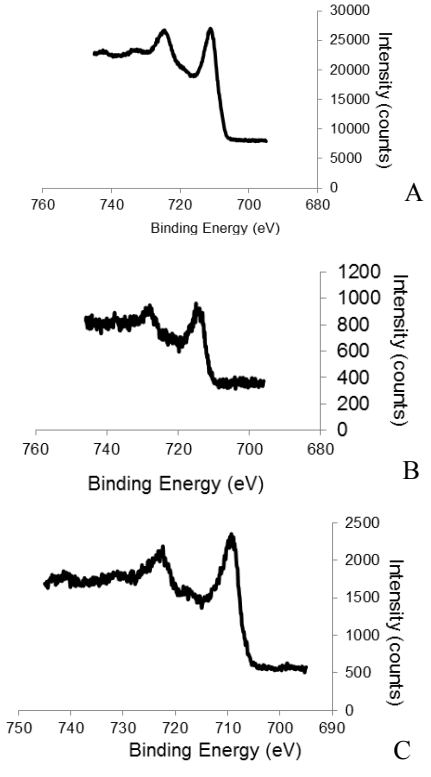

Figure 2. X-ray photoelectron spectra in the Fe 2p binding energy region for commercial maghemite particles (1a), AP003 particles (1b) and AP013 particles (1c).

Transmission electron microscopy (TEM) was used to obtain images of the iron oxide nanoparticles. In Fig. 3 and Fig. 4 are images of AP013 and AP020 particles. These images were typical in that the particles obtained under all reaction conditions where spherical. The vast differences in particle diameter and particle size distribution can be seen in the variations between the TEM images. The particle size distribution for AP018 was much narrower than the distribution for AP020.

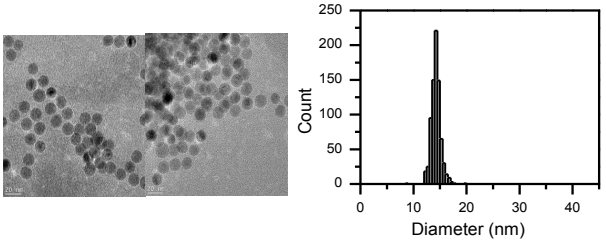

Figure 3. TEM images of iron oxide particles from AP018 and a histogram showing the particle size distribution. A total of 782 particles were counted. The aver-

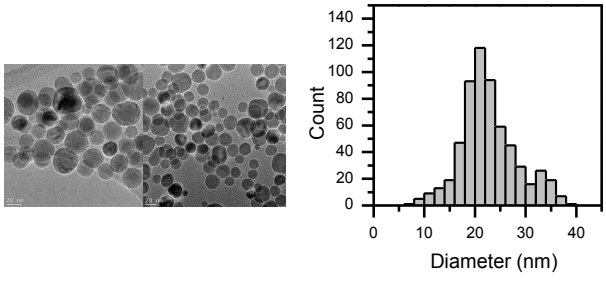

Figure 4. TEM images of iron oxide particles from AP020 and a histogram showing the particle size distribution. A total of 601 particles were counted. The average

Varying the reaction conditions of the iron oleate decomposition reaction allows the size and shape of the magnetite nanoparticles to be altered [5]. The effect of two variables, reaction solvent and reaction time, on the size and composition of the nanoparticles was studied.

Sample	Solvent	Reaction Time (min)	TEM Diameter (nm)
AP003	Benzyl Ether	30	7 ± 1
AP013	Benzyl Ether	30	11 ± 2
AP015	Octadecene	30	21 ± 4
AP018	Octadecene	45	14.3 ± 0.9
AP019	Octadecene	60	18 ± 9
AP020	Octadecene	75	23 ± 6

Table 1. Effect of the reaction conditions on the particle diameter and distribution of particle diameters

The use of benzyl ether in this reaction produced particles with a diameter of 7-11nm, and the use of 1-octadecent produced particles with diameters ranging from 14.3-23 nm with a large size distribution when reacted at the conditions specified in Table 1. While AP003 and AP013 were made with the same reaction solvent and were refluxed for the same amount of time, the diameters are very different. When synthesizing AP013, technical difficulties occurred while heating to reflux temperature. As a result, the reaction was left at 100°C for 2 hours before continuing to heat and then remained at reflux for 30 minutes. The rate at which the nanoparticle reaction heats to reflux temperature is a possible variable contributing to this size change. As evident in the size differences in AP013 and AP003, the heating rate sometimes cannot be controlled well. Additionally, the transition of magnetite to maghemite and decomposition of iron oleate mechanisms are not completely understood. Thus, analyzing the specific chemical and property changes based on varying reaction conditions and drawing concrete conclusions proves to be difficult.

While particle diameter tended to increase with longer reaction times, the particle size distribution greatly fluctuated. Ideally, particles will be optimized to one diameter size with a small size distribution allowing the entire batch to heat similarly. The optimal synthesis procedure will be determined in future work. Obtaining SAR values on particles of different sizes will provide data on the particles with the best diameter for effective heating. Once this is determined, batches will be replicated and heating experiments repeated in order to accurately and repetitively synthesize particles with a reasonable size distribution to be used in the drug delivery system.

Conclusion

Magnetic nanoparticles have an exciting future of application to biomedical fields and research in a variety of areas. As the core of the drug delivery system, iron oxide magnetic nanoparticles must be optimized for the human body, as well as for drug delivery through magnetic induction heating. The optimization of these particles is determined by analyzing the properties, including size distribution and heating efficiency, at different particle sizes. Reaction solvent and reaction temperature both contribute to the change in nanoparticle diameter. This experiment examined iron oxide nanoparticles synthesized under two reaction solvents, benzyl ether and 1-octadecene, and the 1-octadecene particles at four different reaction times: 30, 45, 60, and 75 minutes. Changes in particle diameter and size distribution were observed, indicating that the changes made successfully altered the composition of the nanoparticles. Future work will be done to further consider the optimization of these particles through replication and heating experiments.

References

[1] Cervlino A, Grison G, Cerrito A, Guagliardi A & Masciocchi N. (2014). Lattic Parameters and Site Occupancy Factors of Magnetite-Maghemite Core-Shell Nanoparticles. A critical study. J. Appl. Cryst. 47:1755-1761.

[2] Lu AH, Salabas EL, and Schüth F. (2007). Magnetic Nanoparticles: Synthesis, Protection, Functionalization, and Application. Angewandte Chemie International Edition, 46: 1222–1244.

[3] Park J, An K, Hwang Y, Park JG, Noh, HJ, Kim, JY, Park, JH, Hwang, NM & Hyeon, T. (2004). Ultra-large scale syntheses of monodisperse nanocrystals. Nature Materials 3: 891-895.

[4] Siegel RL, Miller KD, & Jamal A. (2016). Cancer Statistics 2016. CA: A Cancer Journal for Clinicians, 66:7-30.

[5] Sun S & Hao H. (2002). Size Controlled Synthesis of Magnetic Nanoparticles. J. Am. Chem. Soc., 28: 8204-8205.

[6] Sun S, Zeng H, Robinson DB, Raoux S, Rice PM, Wang SX, & Li G. (2004). Monodisperse MFe2O4 (m=Fe, Co, Mn) Nanoparticles. J. Am. Chem. Soc. 126:273-279.

[7] Yamashita T & Hayes P. (2008). Analysis of XPS Spectra of Fe2+ and Fe3+ in Oxide Materials. Appl. Surf. Sc. 254:2441-2448.

Synthesis of α-FeOOH and CoP_i Thin Films for use as Catalysts in Electrochemical Water Oxidation and Efficiency Comparison to Known Effective Catalysts

Jeremy Hitt, Dusty Trotman; Shanlin Pan, Ph.D.

Faculty Mentor: Shanlin Pan

Department of Chemistry, The University of Alabama, Tuscaloosa, AL, 35487

As the world looks to develop new forms of clean, renewable energy, water oxidation by electrolysis appears very promising. Electrolysis is used to produce hydrogen and oxygen gas which is combusted in fuels cells to make electricity. The most important factor affecting the efficiency of electrolysis cells is the electrode surface that is in contact with the water. Here we synthesize, test, and compare two newer types of catalysts for water splitting that can perform at near neutral pH. These two catalysts, α-FeOOH and CoP_i, are grown on conductive glass surfaces by electrodeposition and compared with two previously known catalysts (IrO_x nano-particle thin film and NanoCOT). The samples are used to split water in an electrochemical cell using linear sweep voltammetry, and their efficiencies are calculated and compared graphically to assess their effectiveness for large scale hydrogen

Introduction

As the amount of greenhouse gases in the atmosphere continues to rise, the push to power the planet with clean renewable energy sources must increase as well. The sun produces an enormous amount of energy for us to use in the form of radiation, making solar energy a viable source to power the planet. The largest problem with using solar

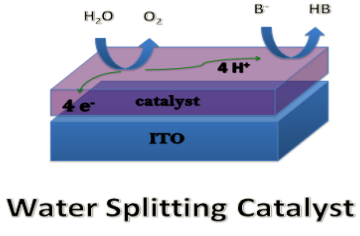

Figure 1. Schematic of catalyzed water oxidation half reaction at a catalytic material prepared on top of an indium-tin-oxide (ITO) electrode.

energy is the lack of sunlight at night and unfavorable climates that experience frequent cloud coverage. To make solar energy effective, excess energy must be collected and stored during the day to use at night. Large scale energy storage is a difficult task and one of the most promising ways to store large amounts of energy is to break H_2O molecules into more energetic H_2 gas by artificial photoelectrochemical systems [1]. H_2 gas can then be combusted or used as fuel of a hydrogen fuel cell at a later time to release the energy when it is needed and does not produce any greenhouse gases as a byproduct. The simplest and most cost effective way to split water molecules is by a photoelectrochemial oxidation/reduction reaction in a solution of water containing an electrolyte where an electric potential difference is supplied by light absorbing semiconductor materials or a solar cell panel. If the potential difference is high enough to force electrons off of the molecules in solution then a current is passed through the solution, and H_2 and O_2 gas bubbles out of the solution by following the two half reactions:

Reduction at cathode in base:

$$2\ H_2O(l) + 2\ e^- \rightarrow H_2(g) \cdot 6\ OH^-(aq)$$

Oxidation at anode in base:

$$4\ OH^-(aq) \rightarrow O_2(g) \cdot 6\ H_2O(l) + 4\ e^-$$

There are several factors that contribute to the efficiency of the water splitting reactions, but what affects the efficiency the most is the surface of the electrode that is in contact with the solution (Figure 1). Catalysts are often used to increase the efficiency of water splitting and poor catalysts require a high over potential to force the reaction to happen which is undesirable for large-scale production. Many compounds are unstable in the environment required for water splitting, and frequently replacing them is economically unfeasible. Furthermore, the material must be relatively cost effective in order to be affordable for use on large scale. With all these factors in mind, two different compounds were chosen to test their properties for potential use as catalysts for water splitting in an electrochemical cell. The first compound tested was α-FeOOH which was chosen because its similarity to a known catalyst (α-Fe_2O_3), and the abundance of Fe on the earth makes this material cheaper than ones containing more rare elements. Also it has been reported that α-FeOOH can be used in EC cells with a near-neutral pH as opposed to very caustic solutions used with other materials [2]. The second

pound tested was CoP_i which was also chosen because of its stability and activity at near neutral pH [4]. Few catalysts that perform well at neutral pH are known to exist which makes these new catalysts safer to use and a good prospect for large scale H_2, O_2 fuel production.

Materials and Methods

α-FeOOH [2] The thin film catalyst was electrodeposited on the working electrode of fluorine-doped tin oxide (FTO) coated glass (ACE Glass Inc.) with an electrochemical cell using a BASi Epsilon potentiostat (Figure 2).

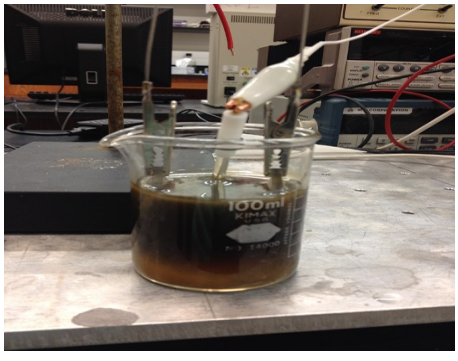

Figure 2. Electrochemical cell containing Fe^{2+} electrolytic bath used for cyclic voltammetry and depositing α-FeOOH thin films of FTO.

The glass was cleaned with soap and deionized water before being placed in the electrolyte solution. The counter electrode was inert graphite and was held ~45 cm away from the working electrode. The electrodepostion was done at a steady potential of -0.2 V vs. Ag/AgCl (1 M KCl) reference (CH Instru**Figure**

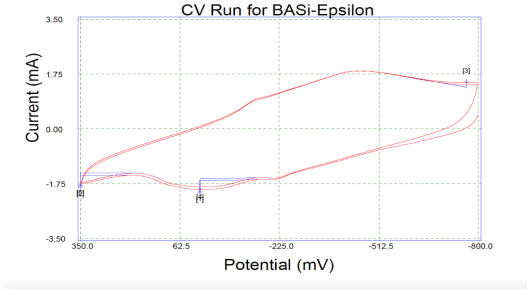

Figure 3. Cyclic voltammogram of Fe^{2+} solution used to determine the optimal deposition potential for FeOOH.

ments). The electrolyte bath was prepared by mixing 70 mL of 0.4 M NaCl (Fischer Scientific) with 1.25 mL of 0.5 M $FeCl_2$ (Alfa Aesar). Next 0.574 g (0.6 mL) of neat N-methylimidazole (Tokyo Chemical Industy Inc.) was added to the solution and quickly stirred. It is important to quickly add the final solution to the EC cell because in the air it will oxidize quickly and the solution is no longer suitable for thin film deposition after about 2 hours. Cyclic voltammetry was used first to determine the optimal potential for electrodepostion of FeOOH by scanning a potential range from -0.80 V to 0.35 V as shown in Figure 3. Samples were grown for variable amounts of time at a constant potential of -0.2 V to determine roughly the optimal deposition time of the thin film for water splitting. All the samples were grown with a surface area of 1.5 cm^2 except the 1 hour thickness which was 2 cm^2.

CoP_i [4] A 100 ml phosphate buffer was prepared by mixing 1.379 g KH_2PO_4 (Amresco) and 0.3997 g NaOH (VWR) to make 0.1M potassium phosphate at pH 7.0. An electrolytic bath was prepared by mixing 50 mL of 0.1M potassium phosphate buffer pH 7.0 with 50 mL of 0.5 mM of $Co(NO_3)_2$. Graphite was used as a counter electrode at a distance of 45 cm from an Indium tin oxide coated glass (ITO) working electrode within the electrolytic bath. Next, we designated an optimal deposition potential through the process of cyclic voltammetry (BASi Epsilon) at a scan rate of 100 mV/sec. The cyclic voltammetry technique was set for a double sweep from -0.2 V to 1.2 V in the 0.5 mM solution of $Co(NO_3)_2$ in 0.1 M potassium phosphate pH 7.0. As shown by Figure 4, we found the potential of 1.093 V vs. Ag/AgCl (1.0 M KCl) reference (CH Instruments) was optimal. Then, an ITO electrode (Ace Glass) was cleaned using distilled water and soap. The electrodepositions (BASi Epsilon) of the films were performed at constant potentials of 1.093 V vs. Ag/AgCl (1.0 M KCl) references (CH Instruments). Then the CoP_i film was grown onto an ITO electrode using 1.093 V for different intervals of time to obtain films of variable thickness. We chose the time intervals of 30 minutes, 1 hour, and 3 hours to compare the efficiency of different thickness for water splitting and each film had a surface area of 1.5 cm^2.

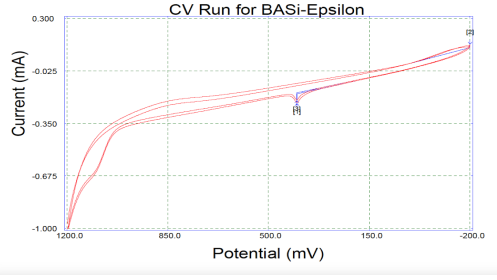

Figure 4: Cyclic voltammogram of Co^{2+} solution used to determine the optimal deposition potential of CoP_i.

IrO_x [6] The thin films were prepared on cleaned FTO

coated glass in an EC cell using a BASi Epsilon potentiostat with a graphite counter electrode. First, IrO_x nanoparticles were synthesized by heating 2.4 mM K_2IrCl_6 at 90°C for 20 minutes at a pH of 13. The solution is immediately cooled by placing it in an ice-bath for 15 minutes. A blue solution of IrO_x nanoparticles is formed and used as a bath for electrodepostion onto FTO by applying a steady potential of 1.0 V vs. Ag/AgCl (1 M KCl). One sample was grown for 30 minutes and another was grown for 1 hour to produce variable thicknesses to test for their catalytic water splitting efficacies. Each film was immersed in the solution enough to deposit a film with a surface area of 1.5 cm^2.

NanoCOT [6] A 0.5 cm^2 coated titanium electrode was synthesized in the Pan lab group by the procedure described by Shan et al [6]. The electrode was also tested in an electrolysis cell to compare with the efficiency of the other materials.

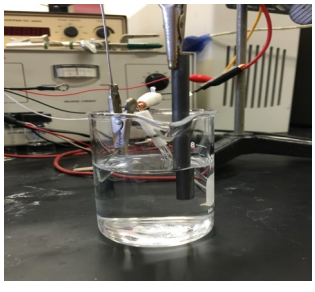

Figure 5. Electrochemical cell used to deposit thin films and test their catalytic efficiencies for water splitting.

Each sample made was tested for its efficiency to oxidize water into oxygen gas in an electrochemical cell. For the water oxidation tests, the counter and reference electrodes and thin film samples were dipped in a 70 mL solution of phosphate buffer (pH 7.0) as seen in Figure 3. A variable potential of 0.0 V -1.6 V was applied by a potentiostat with a scan rate of 100 mV/s to obtain a cyclic voltammogram.

Results

The measurements obtained by the electrochemical water splitting are graphed by -ln|(-current (mA))/ cm^2| vs. potential (V), and a linear trend line was fitted to the stable region of potentials to extrapolate the relative exchange current and slope of each sample film. The graphs showing the relationships of current density vs. potential for each type of catalyst tested are shown in Figures 6-10, and the slope and y-intercept of each line is listed in Table 1 for comparison.

Catalyst	Time	Slope ln(-mA/cm^2)/V	Intercept ln(-mA/cm^2)	R^2
α-FeOOH	10 minutes	11.96	24.94	0.88538
	20 minutes	8.60	19.57	0.97534
	30 minutes	10.90	22.92	0.92635
	1 hour	12.18	24.74	0.90361
IrO_x	30 minutes	3.11	10.57	0.93195
	1 hour	2.48	12.49	0.93029
ITO	-	1.19	12.15	0.91180
Nano-COT	20 minutes	2.72	9.18	0.89726
CoP_i	30 minutes	10.80	21.89	0.95347
	1 hour	13.19	24.68	0.91812
	3 hours	13.30	24.02	0.92988

Table 1. Comparison of Different Water-Splitting Catalyst Efficiencies.

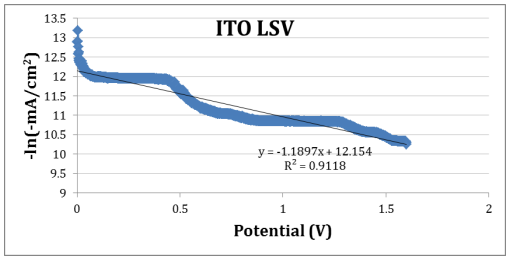

Figure 6. Indium tin oxide coated glass was used as a blank electrode in an electrolysis cell containing phosphate buffer (pH 7) to show the current produced without a catalyst.

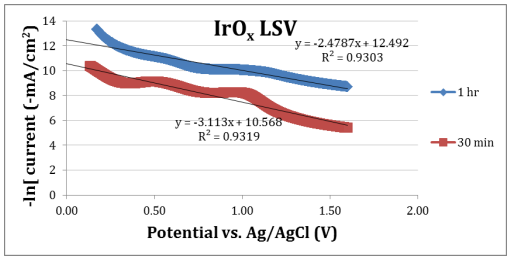

Figure 7. Electrolysis with iridium oxide nanoparticles deposited of FTO coated glass in electrochemical cell for 30 minutes and 1 hour vs. Ag/AgCl reference.

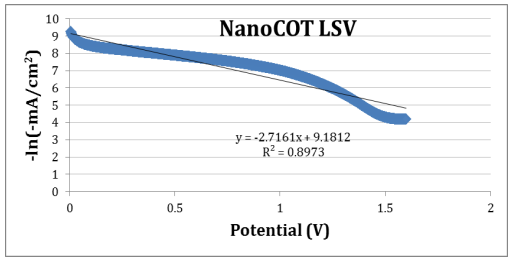

Figure 8. Electrolysis with NanoCOT coated titanium electrode synthesized in the Pan lab according to the procedure reported by Shan et al [6].

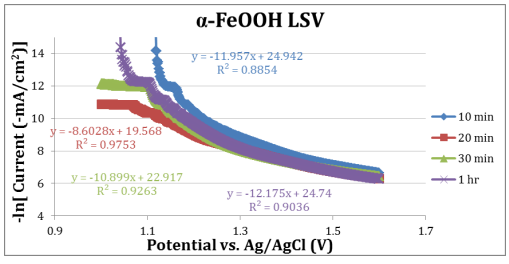

Figure 9. Linear sweep voltammogram of the stable region of water oxidation in an electrochemical cell containing phosphate buffer (pH 7) and α-FeOOH catalyst.

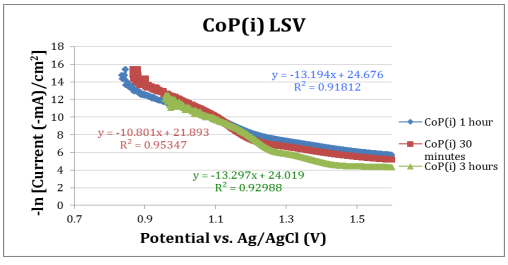

Figure 10. Linear sweep voltammogram of the stable region of water oxidation in an electrochemical cell containing phosphate buffer (pH 7) and CoP_i catalyst.

Discussion

Water splitting is a kinetically and thermodynamically difficult process. Two water molecules must be oxidized to make one molecule of oxygen which requires four holes (or oxidizing equivalents), and is dependent upon the presence of catalytic sites to enable this multi-electron chemistry [3]. In order to quantitatively compare the efficiency of the catalysts tested, the slopes and y-intercepts of the fitted trend lines are used to show how quickly the current increases on a given voltage interval and the exchange current density respectively. The current density-voltage characteristic of the catalyst is a key determinant of the solar-to-fuel efficiency [7].

The results show that the FeOOH preformed best for deposition times of 10 minutes and 1 hour while the CoPi preformed best when grown for 1 hour or more. The average exchange current density at 0 V over potential for all FeOOH samples is denoted by the y-intercepts and has a value of 23.042 (ln[-mA/cm2]) while CoPi was slightly higher at 23.529 (ln[-mA/cm2]). It is clear that both of the new materials performed significantly better in the range chosen than bare ITO, IrOx thin films, and the NanoCOT coated electrode. The average slope recorded for FeOOH was 10.908 (ln[-mA/cm2]/V) and for CoPi the average slope was even higher at 12.431 (ln[-mA/cm2]/V). IrOx had an average slope of 2.796 (ln[-mA/cm2]/V) and y-intercept of 11.530 (ln[-mA/cm2]) while the NanoCOT had a slope of 2.716 (ln[-mA/cm2]/V) and y-intercept of 9.181 (ln[-mA/cm2]). This confirms that both of the new catalysts performed more efficiently than the IrOx and NanoCOT catalysts in the voltage ranges that were compared. It is important to note that the stable linear range for the FeOOH and CoPi is much smaller than for IrOx and NanoCOT. The FeOOH has a stable range from 1.1 to 1.6 V and CoPi from 0.9 to 1.6 V while the IrOx and NanoCOT are virtually stable from 0.0 to 1.6 V.

The predicted advantage of the FeOOH and CoPi is their high efficiency at near neutral pH which greatly diminishes the efficiency of the IrOx and NanoCOT. Along with their lower cost and toxicity, α-FeOOH and CoPi show very high potential as use for large-scale electrochemical water oxidation catalysts for the production of hydrogen gas, and a clean, renewable energy source.

References

[1] Alibabaei L, Brennaman MK, Norris MR, Kalanyan B, Song W, Losego MD, Concepcion JJ, … & Meyer TJ. (2013). Proceedings of the National Academy of Sciences of the United States of America, 110:20008-20013.

[2] Chemelewski WD, Lee HC, Lin JF, Bard AJ, & Mullins BC. (2014) Amorphous FeOOH oxygen evolution reaction catalyst for photoelectrochemical water splitting. Journal of the American Chemical Society, 136:2843-2850.

[3] Dau H, et al. (2010). The mechanism of water oxidation: From electrolysis via homogeneous to biological catalysis. ChemCatChem, 2:724-761.

[4] Kanan MW, & Nocera DG. (2008). In situ formation of an oxygen-evolving catalyst in neutral water containing phosphate and Co2+ . Science, 321:1072-1075.

[5] Seabold JA & Choi KS. (2012). Efficient and stable photo-oxidation of water by a bismuth vanadate photoanode coupled with an iron oxyhydroxide oxygen evolution catalyst. Journal of the American Chemical Society, 134:2186-2192.

[6] Shan Z, Archana PS, Shen G, Gupta A, Bakker MG, & Pan S. (2015). NanoCOT: Low-cost nanostructured electrode containing carbon, oxygen, and titanium for efficient oxygen evolution reaction. Journal of the American Chemical Society, 137:11996

[7] Surendranath Y, Bediako DK, & Nocera DG. (2012). Interplay of oxygen-evolution kinetics and photovoltaic power curves on the construction of artificial leaves. Proceedings of the National Academy of Sciences of the United States of America, 109:15617-15621.

About the Authors

Jeremy Hitt is a senior at The University of Alabama. He is originally from Birmingham, AL and is currently studying Chemistry and Physics. In addition to his work in Dr. Shanlin Pan's research group in the Chemistry department at Alabama, he is a member of the Student Chapter of the American Chemical Society at the University of Alabama and the university's chemistry honors society Gamma Sigma Epsilon.

Dusty Trotman is a senior at The University of Alabama. He is originally from Fort Payne, AL and is currently studying Biology with a Chemistry minor. Along with his work in Dr. Shanlin Pan's research group in the Chemistry department at Alabama, he is a member of the Phi Sigma Theta National Honors Society and also the Society for Collegiate Leadership and Achievement Honors Society.

Construction and Characterization of p-type heterojunction CuO|CuBi2O4 photocathode electrode for photoelectrochemical reduction of water as sustainable source of energy

Kieran Bhattacharya and Qamar Tejani
Department of Chemistry, The University of Alabama, Tuscaloosa, AL 35487

CuO|CuBi2O4 is a promising p-type semiconductor that can be potentially applied to transparent solar water splitting because of its low cost and visible light sensitivity. Herein we investigated the effect of sample preparation conditions on water reduction activities under visible light irradiation. This conditions include nanowire concentration, nanowire deposition layering, deposition method, and electrode base material. Our findings support the theory that the heterojunction's optimal photocurrent can be produced by preventing overcrowding of photocathode material and depositing the precursor solutions by drop-casting the layers onto optically transparent indium doped tin oxide (ITO) or fluorine doped tin oxide (FTO) electrodes.

Introduction

Recent studies show that we will likely deplete earth's reserves of oil, coal, and gas within 100 years [1]. Therefore there is an urgent need to find efficient, low-cost alternative energy harvesting and conversion systems. Among these, solar cell applications as a primary source of energy needs hold the promise to provide clean and low cost alternative energy if their efficiency can be increased with decreased cost for more broad usage. In the first 7 months of 2015, 82% of the 58 quadrillion Btu consumed by Americans was supplied by fossil fuels; whereas, solar applications only provided 0.54%, nearly 9 times its rate in 2005 [2]. While solar energy has become an increasingly popular investment because of its sustainability and environmental friendliness, the cost of application materials and installation remain too expensive to supply all or most of individuals' energy consumption.

Another potential challenge for solar energy technology is storage. Solar cells used for electrolysis have been implemented for over 40 years [3] to store energy into chemical bonds. These devices generate electrical current by absorbing photons to excite electrons on electrode surfaces via the photovoltaic effect; solar cells thus convert light energy to electrical potential energy, which can then drive chemical reactions to store energy. Semiconductor materials are used for harvesting sunlight and storing energy by photochemical reactions. Such photoelectrochemical systems are very much dependent on the composition, morphology, and spatial configuration of the interfaces under visible light irradiation, while clean fuel cells such as hydrogen are artificially produced to minim photosynthesis.

These semiconductor materials are distinguished by those which operate using electrons as majority carriers and holes as minority carriers or holes as majority carriers and electrons as minority carriers, denoted as n-type and p-type respectively. Holes are positions in the semiconductor lattice that lack electrons but can potentially bear them; these can represent mobile, positive charges. While most research of surface modifications for solar water splitting has been into n-types, such as TiO2 [4], Ga2O3|Cu2O [5], ZnO|Cu2O [6], In2O2|Cu2O [7], TiO2|Cu-Ti-O [8], TiO2|Cu2O [9], p-types have still been well-studied and include Cu2O [5, 10], CuO [11], and the heterojunction of interest, CuO|CuBi2O4.

Both CuO and CuBi2O4 have been independently investigated in solar water splitting [11, 12]. CuO forms a p-type monoclinic crystal system with a square planar configuration and attractively small band gap. CuBi2O4 forms a tetragonal structure with a band gap of approximately 1.7 eV. Together, CuO|CuBi2O4 have a band gap of approximately 1.4-1.6 eV and create a p-type heteropolymer; moreover, the structure has been shown to perform significantly higher photocurrent efficiencies under linear sweep voltammetry with respect to CuO and CuBi2O4 independently [13].

Figure 1. Diagram of FTO|CuO|$CuBi_2O_4$ photocathode

The intention of this study is to investigate and analyze four aspects of CuO|$CuBi_2O_4$ performance in solar cell water reduction to produce hydrogen: the concentration of precursor; the number of deposited coating layers; the coating method effect of drop-casting and spin-coating of the precursor solution onto the surface electrode; and the type of surface electrode, either indium tin oxide (ITO) or fluorine-doped indium tin oxide (FTO), both of which are optically transparent and electrically conductive. Based on previous studies with other p-type semiconductors [5, 10, 11, 12, 13], it is expected that densely packed semiconductor film will reduce the photocurrent efficiency; whereas, a coverage of semiconductor material that is too scarce or not completely covering the irradiated surface will render the electrode ineffective. It is expected that applying multiple layers of precursor solution onto the electrode will be less efficient than applying the same amount of solution in one drop-cast or spin-coat because one deposition should produce a more uniform surface layer. It is expected that deposition by spin-coating will produce a more uniform CuO|$CuBi_2O_4$ layer than by drop-casting because of Brownian motion of the dissolved precursor solute in solvent while the solvent is vaporized off of the electrode surface. Finally, it is expected that CuO|$CuBi_2O_4$ layers deposited on FTO electrodes will perform better than layers deposited on ITO electrodes because the fluorine doping is expected to increase the electrode's majority carrier concentration [14].

Materials and Methods

CuO|CuBi2O4 thin film electrodes were constructed by drop-casting varying amounts of 10 mM $Cu(NO_3)_2{\cdot}3H_20$ for CuO and 2 mM $Cu(NO_3)_2{\cdot}3H_20$ with 4 mM $Bi(NO_3)_3{\cdot}5H_2O$ for $CuBi_2O_4$, all of which in ethylene glycol solution, on cleaned FTO and ITO glass. Slides were cleaned for 15 minutes via sonication using 3 treatments of DI water, and 1 treatment of acetone and isopropanol. After the slides were dried off with nitrogen gas, UV/Ozone treatment was applied to clean the surface of the slides. Both FTO and ITO coated glass were measured precisely at 1.5 x 1.5 cm^2. When coating the slides, 75 µL and 168 µL of the precursor solutions were placed on the slides at room temperature to determine differences in photocurrent efficiency based on the amount and placement of nanowires on the slides. The slides were then carefully treated with 1 to 2 layers of the precursor solutions to identify differences in morphology based on differences in layering.

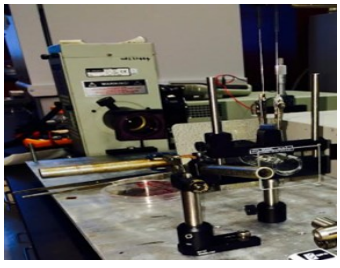

Figure 2. Lamp and electrochemistry cell used for characterization of photocathodes.

Between each coating, the slides were placed in the oven for 30 minutes at 150 °C to evaporate the solvent and deposit the semi-conductive films. After the slides were completed with treatment from the precursor solutions, they were annealed for 3 hours at 500 °C. The samples were then analyzed by morphology, linear scanning voltammetry (LSV), and amperometric i-t curves. Linear scanning voltammetry and amperometry were inspected for both FTO and ITO coated glass. Analysis of LSV required the potential to range from 0.30 V to 0 V. Furthermore, the scan rate was set to 0.05 V/s, and sensitivity was set to 0.001 A/V. Amperometric i-t curves were analyzed for 60 seconds with sensitivity set at 0.001 A/V as well. Current for each subset of tested electrodes was then measured for the allotted time.

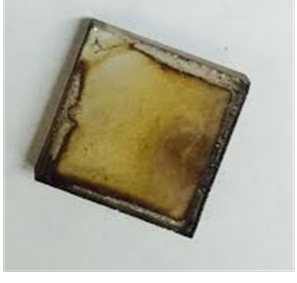

Figure 3.
FTO|CuO|$CuBi_2O_4$

Results

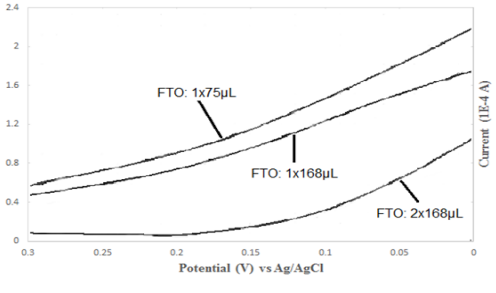

Figure 4. LSV sweeps of FTO with 1x75 µL, 1x168 µL, 2x168 µL drop-casts.

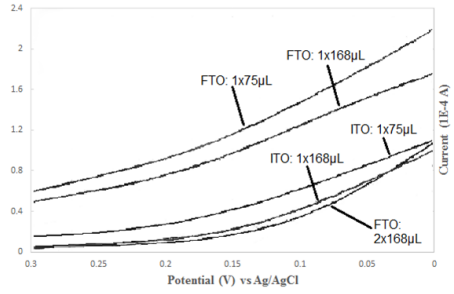

Figure 5. LSV sweeps of ITO with 1x75 µL, 1x168 µL and FTO with 1x75 µL, 1x168 µL, 2x168 µL drop-casts. Scan rate: 0.05 V/sec.

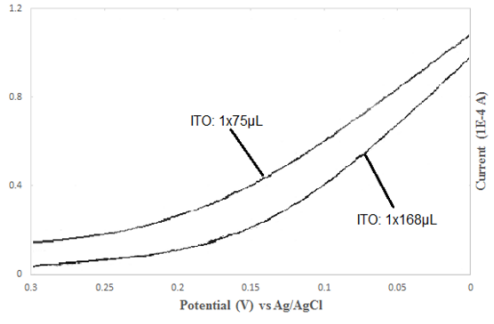

Figure 6. LSV sweeps of ITO with 1x75 µL, 1x168 µL drop-casts. Scan rate: 0.05 V/sec.

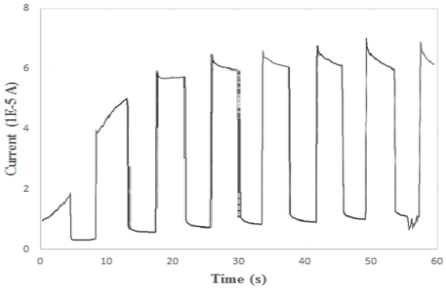

Figure 7. Amperometric i-t curve of FTO|CuO|$CuBi_2O_4$ with 1x75 µL drop-cast.

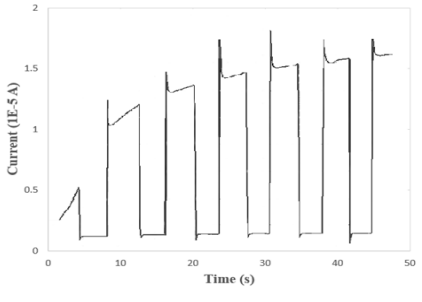

Figure 8. Amperometric i-t curve of FTO|CuO|$CuBi_2O_4$ with 2x168 µL drop-cast.

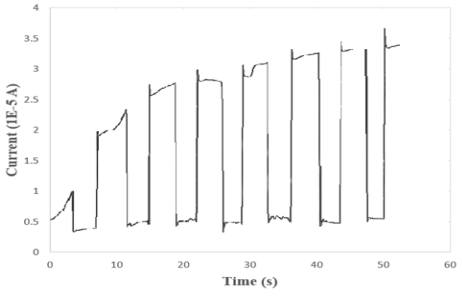

Figure 9. Amperometric i-t curve of ITO|CuO|$CuBi_2O_4$ with 1x75 µL drop-cast.

Discussion

Based on the results from linear scanning voltammetry (LSV) and amperometric i-t curve tests, the concentration of surface coating condition was found to have significant effects on the photocurrent efficiency of the electrodes on both ITO and FTO substrate. Photocurrent density of FTO|CuO|CuBi2O4 electrodes prepared with one dropcast of 75 µL precursor solution produced noticeably better current flow than the same electrode prepared with one drop-cast of 168 µL precursor solution. Moreover, in the LSV testing, ITO|CuO|CuBi2O4 prepared from a 75 µL drop-cast solution performed significantly better than the same electrode prepared with one drop-cast of 168 µL precursor solution. Also, the FTO|CuO|CuBi2O4 prepared with 75 µL rendered nearly four times the peak current in their respective amperometric i-t curves. This data supports the theory that a drop-cast deposition of 168 µL precursor solution led to an unfavorably high-density packing of CuO|CuBi2O4 on both the ITO and FTO surface electrodes, which resulted in a reduction of each sample's photocurrent efficiency.

In addition, the layering of drop-casts was found to affect the photocurrent efficiency of the FTO substrate. The LSV sweeps of FTO|CuO|CuBi2O4 with 2 drop-casts of 168 µL precursor solution exhibited significantly worse current output with respect to the FTO|CuO|CuBi2O4 electrode with 1 drop-cast of 168 µL precursor solution. Along with the fact that 2 drop-casts produce a less favorably density of semiconductor material on the electrode, the act of drop-casting multiple layers as opposed to a single deposition resulted in less uniform film on the surface. This deviation in uniformity was easily noticeable by visual analysis of the respective films after annealing and cooling of the electrodes. The reason for this is quite

simply that the first of the two drop-casts created a non-uniform surface on the uniformly deposited FTO because of the Brownian motion of the solute in the solvent as the solvent is being vaporized off of the electrode surface, so the second drop-cast is expected to create a less uniform film in that it is being deposited onto a surface that is already not completely uniform.

The FTO|CuO|CuBi2O4 electrodes prepared by spin-coating as opposed to drop-casting the precursor solution was found to produce a more uniform film. This was expected because the centrifugal force of the solution on the spin-coater was meant to counteract the random motion of solute particles in the solvent to more evenly distribute the nanowires on the electrode surface. However, a comparative quantification of the photocurrent efficiency between the electrodes prepared by spin-coating and drop-casting was impractical and not carried out because it would be very difficult to accurately quantify how much of the initial precursor solution was deposited on each spin-coated electrode and drop-cast an equivalent amount on a separate electrode. Thus, it would be inappropriate to compare electrodes by LSV or amperometric i-t curves when each sample would have different morphologies, which would in itself affect how well each sample performs under both tests.

CuO|CuBi2O4 nanowires deposited on FTO electrodes outperformed those deposited on ITO electrodes. The photocurrent of FTO|CuO|CuBi2O4 samples prepared with 1 drop-cast of 75 µL and 168 µL precursor solution was significantly higher than the respective ITO|CuO|CuBi2O4 samples prepared with the same amount of precursor solution. Furthermore, the FTO|CuO|CuBi2O4 samples prepared with 1 drop-cast of 75 µL exhibited nearly twice the peak current of ITO|CuO|CuBi2O4 with the same precursor solution. The increased output of the FTO samples supports the idea that fluorine-doping can increase the majority charge carrier mobility of ITO.

Conclusion

Ultimately, the goal of this investigation was to analyze $CuO|CuBi_2O_4$ photocurrent efficiency for solar water reduction in four areas: the effect of precursor concentration; the number of deposited coating layers; the coating methods of both drop-casting and spin-coating the precursor solution onto the surface electrode; and the type of surface electrode, either ITO or FTO. Data from linear scanning voltammetry, amperometric i-t curves, and analysis of morphology supported the following notions: the drop-cast of 168 µL precursor for both $FTO|CuO|CuBi_2O_4$ and $ITO|CuO|CuBi_2O_4$ led to an unfavorably high-density packing of $CuO|CuBi_2O_4$ nanowires, leading to lower photocurrent efficiency than a 75 µL drop-cast onto ITO and FTO; adding multiple layers of a drop-casted solution led to lower photocurrent efficiency for the electrode due to over-packing and non-uniform distribution of $CuO|CuBi_2O_4$ layer; spin-coating the precursor solution created a more evenly distributed set of $CuO|CuBi_2O_4$ nanowires on the electrode surface, but comparison between each deposition method's photocurrent efficiency was impractical due to the difficulty of applying a consistent concentration of nanowires on both sample sections; FTO served as a better electrode surface to deposit $CuO|CuBi_2O_4$ than ITO due to the fluorine-doping ability to increase the majority charge carrier mobility of ITO.

While $FTO|CuO|CuBi_2O_4$ serves as a promising electrode composition for solar water splitting, much more inquiry can be done to improve the efficiency of the current deposition methods or to investigate new deposition methods. Coating the $FTO|CuO|CuBi_2O_4$ heterojunction with catalytic materials for production reduction (e.g. platinum) might further improve the photocurrent. Also, depositing the precursor solution onto the electrode using a spray gun could provide a quicker method of creating the nanowires and produce a more even distribution; however, as with spin-coating, problems might arise in quantification of semiconductor deposited onto the electrode surface and comparing photocurrent performance of a particular spray gun sample with respect to drop-casted samples.

References

[1] Apergis N, Payne JE. (2011). Renewable and Non-Renewable Energy Consumption-Growth Nexus: Evidence from a Panel Error Correction Model. Energy Economics. 34: 733-738.

[2] U.S. Energy Information Administration. (2015). Energy Overview. 7.

[3] Fujishima, A.; Honda, K. 1972. Electrochemical Photolysis of Water at a Semiconductor Electrode. Nature. 238:37.

[4] Khan SUM, Al-Shahry M, Ingler Jr. WB. (2002). Efficient Photochemical Water Splitting by a Chemically Modified n-TiO2. Sci., 297: 2243.

[5] Minami T, Nishi Y, Miyata T. (2013). High-Efficiency Cu2O-Based Heterojunction Solar Cells Fabricated Using a Ga2O3 Thin Film as N-Type Lay-

er. Appl. Phys. Express. 6: 041101

[6] Minami T, Nishi Y, Miyata T, Nomoto J. (2011). High-Efficiency Oxide Solar Cells with ZnO/Cu2O Heterojunction Fabricated on Thermally Oxidized Cu2O Sheets. Appl. Phys. Express. 4: 062301.

[7] Mittiga A, Salza E, Sarto F, Tucci M, Vasanthi R. (2006). Heterojunction solar cell with 2% efficiency based on a Cu2O substrate. App. Phys. Lett. 88: 1-2

[8] Mor GK, Varghese OK, Wilke RH, Shama S, Shankar K, Latempa TJ, Choi KS, Grimes CA. (2008). p-Type Cu-Ti-O Nanotube Arrays and Their Use in Self-Biased Heterojunction Photoelectrochemical Diodes for Hydrogen Generation. Nano Lett. 8.7: 1906-1911.

[9] Siripala W, Ivanovskaya A, Jaramillo TF, Baeck SH, McFarland EW. (2002). A Cu2O/TiO2 Heterojunction Thin Film Cathode for Photoelectrocatalysis. Solar Energy Materials & Solar Cells. 77: 229-237.

[10] Yuhas BD, Yang P. (2009). Nanowire-Based All-Oxide Solar Cells. J. Am. Chem. Soc. 131: 3756-3761.

[11] Wijesundera RP. (2010). Fabrication of the CuO/Cu2O Heterojunction Using an Electrodeposition Technique for Solar Cell Applications. Semicond. Sci. Technol. 25: 045015.

[12] Hahn NT, Holmber VC, Korgel BA, Mullins BC. (2012). Electrochemical Synthesis and Characterization of p-CuBi2O4 Thin Film Photocathodes. J. Phys. Chem. 116: 6459-6466.

[13] Park HS, Lee CY, Reisner E. (2014). Photoelectrochemical Reduction of Aqueous Protons with a CuO|CuBi2O4 Heterojunction Under Visible Light Irradiation. Phys. Chem. Chem. Phys. 16: 22462-22465.

[14] Yousaf SA, Ali S. (2009). The Effect of Fluorine Doping on Optoelectronic Properties of Tin-Dioxide (F: SnO2) Thin Films. Coden. JNSMAC. 48: 43-50.

Acknowledgements

We thank the NSF for supporting this research under award OIA-1539035. We also acknowledge the support of The University of Alabama Department of Chemistry for supplying necessary materials and instruments.

About the Author

Kieran Bhattacharya and Qamar Tejani are seniors at the University of Alabama, studying Chemistry and Biochemistry, respectively.

Utilization of Corn Cob by Clostridium tyrobutyricum and Clostridium cellulovorans and Characterization of the Inhibition Factors

Matthew Pate[1], Yichen Guo[1], Jacob Robinson[1], Matthew Miller[1], Ryan Malden[1], Chris Mayhugh[1], Rebecca Beasley[1], Jianfa Ou[1], Margaret Liu[1]*

Faculty Mentor: Margaret Liu

1Department of Chemical and Biological Engineering, University of Alabama, Tuscaloosa, Alabama 35487 USA

n-Biobutanol is an attractive alternative to current petroleum-based fuels. It is similar to these fuels in its blending ability, current system compatibility, and high-energy content. However, biobutanol is superior to petroleum-based fuels in its environmental sustainability. The major issues with producing biobutanol on a large commercial-scale include low yields and a high costs of materials needed for production. Our research has focused on lowering the cost of production. Three studies were conducted to analyze the viability of corn cob as a substrate and the effects of inhibitors on butanol production. The first study analyzed C. tyrobutyricum growth and product formation using corn cob hydrolyte. The second study analyzed the growth and product formation of C. cellulovorans on treated corn cob biomass. The third study examined the effects that furfural and phenol inhibitors have on the growth and product formation of C. tyrobutyricum. C. tyrobutyricum produced the highest concentration of butanol, 3.96 g/L, at the 40% hydrolyte condition. The 10 g/L glucose and 3 g/L pretreated corn cob biomass condition resulted in the formation of the most butyrate, 4.95 g/L, by C. cellulovorans. In the phenol and furfural inhibition study, butanol production decreased by 9% at a concentration of 0.5 g/L furfural and 29% with 0.5 g/L phenol. Butanol production began to decrease rapidly after the concentrations of the inhibitors rose above 0.5 g/L, and production stopped at a concentration of 2 g/L for both inhibitors. Future research will focus on studying various detoxification methods to further improve butanol production and lower cost of production. Future research will also focus on producing butanol using a two strain coculture of C. tyrobutyricum and C. cellulovorans.

Introduction

The biofuel industry has long been dominated by ethanol, however butanol is emerging as a promising alternative to current petroleum-based fuels and other biofuels. This is primarily the result of its ability to provide more energy per unit than ethanol [3]. In 2008, a study conducted by BP and DuPont showed that the energy density of biobutanol is similar to that of unleaded gasoline, therefore proving biobutanol to be a reliable biofuel source [4].

Specific bacteria can be used to produce butanol through biological processes. In particular, species of Clostridium, specifically *C. tyrobutyricum* and *C. cellulovorans,* display much promise in biobutanol production. *C. tyrobutyricum* produces butyric acid along with acetic acid. Acetic acid by-product formation negatively affects the desired process by reducing the yield of biobutanol. In order to increase yield of butyric acid and butanol, a novel mutant strain was constructed for *C. tyrobutyricum* by creation of a butanol synthesis pathway in the ACKKO, ack gene knockout, strain [9]. The mutated strain, *C. tyrobutyricum* ACKKO-adhE2, not only maintained a steady yield of butanol product, but also resulted in a small acetate concentration of 0.47g/L [9]. The mutated plasmid also had a higher tolerance to butyric acid inhibition than the wild type plasmid [7]. By using a plasmid with upregulated butyrate and downregulated acetate pathways, butanol product can be optimized while acetate by-product formation can be significantly reduced.

Butanol can be formed by the biological conversion of lignocellulosic biomass via fermentation. Prior to fermentation, pretreatment of the biomass is necessary to degrade the lignin, which cannot be consumed by the *Clostridium [*1]. When biomass is treated prior to being used by the bacteria, certain acid-base products are produced that inhibit the further production of butyric acid. Common process inhibitors are weak acids, furan derivatives, phenolic compounds, and other sugars like furfural and HMF [1].

Corn cob biomass can be specifically pretreated under acidic or basic conditions, which extracts fermentable sugars and forms previously mentioned process inhibitors that are then utilized during fermentation [1]. The inhibition occurs under the formation of process inhibitors, which decrease intracellular ATP and damage the cell membranes of *Clostridium* species, and ultimately alter the metabolic pathway of the bacteria [1]. The pretreatment has been successfully tested in a genetically engineered Saccharomyces 1400(pLNH33) [2]. Pretreatment is crucial in determining the specific amounts of process inhibitors that will be present in the fermentation, as most are toxic to *Clostridium* species in the same manner as

butanol, and can halt cell growth [1, 5].

The main objectives of this experiment were to test the effects of various concentrations of inhibitors on the growth and product formation of *Clostridium tyrobutyricum* and analyze the viability of corn cob as a substrate in two Clostridium species, C. *tyrobutyricum* and *C. cellulovorans. C. cellulovorans* is a strain proven to be effective in degradation of biomass, and for this purpose it will be used in an attempt to produce biobutanol directly from biomass in a co-culture of both *Clostridia.*

Materials and Methods

Study Summary

Three studies were conducted to analyze the utilization of corn cob biomass by two Clostridium strains and the effects that inhibitors have on Clostridium fermentation. The first study involved a batch fermentation of *C. tyrobutyricum* with different amounts of corn cob hydrolyte. *C. tyrobutyricum* cannot break down the corn cob biomass by itself, which is why it must be hydrolyzed first. The second study involved a batch fermentation of *C. cellulovorans* using calcium hydroxide treated corn cob biomass. *C. cellulovorans* is superior in its ability to degrade biomass, and the calcium hydroxide pretreatment aids in its ability to do this. The third involved batch fermentations of *C. tyrobutyricum* with varying concentrations of two different fermentation inhibitors, furfural and phenol. The batch fermentations in these studies were carried out in sealed serum bottles.

Growth and Product Formation of C. tyrobutyricum on Corn Cob Hydrolyte

These studies were completed to evaluate the potential of corn cob as a substrate for the refinery of butanol and/or butyric acid using either *C. tyrobutyricum* or *C. cellulovorans* as the inoculant. The bottles were inoculated with 5 mL of the bacterial strain being tested.

In the first batch fermentation, different amounts of corn cob hydrolysate were placed in C. tyrobutyricum-inoculated bottles containing CGM medium [6]. The different conditions were as follows: (1) 80% hydrolyte, (2) 40% hydrolyte, (3) 20% hydrolyte, and (4) 0% hydrolyte.

The corn cob hydrolysate was prepared by first suspending corn cob in 2% (v/v) dilute sulfuric acid at a solid loading of 10% (w/v). The mixture was then stirred at room temperature and autoclaved at 121 °C for 60 minutes. After cooling, the pH was balanced to 6.5. The autoclaved liquid hydrolysate was collected by centrifugation and vacuum filtration. It was stored at 4 °C until it was ready to use.

Growth and Product Formation of C. cellulovorans on Treated Corn Cob

A second batch fermentation was also completed using *C. cellulovorans* as the bacterial strain, which was placed with various amounts of pretreated corn cob biomass and glucose. The three conditions were as follows: (1) 20 g/L glucose; (2) 6 g/L pretreated corn cob biomass; and (3) 10 g/L glucose and 3 g/L pretreated corn cob biomass.

To prepare the treated biomass, 10 g of corn cob was first suspended in 100 mL of water in a 500 mL flask. Calcium hydroxide was then added in a loading of 1.5% w/w based on raw materials. The mixture was then placed in an autoclave set at 45 □ for 60 minutes. After cooling, the pH was balanced back to 6.8 using 2 mol HCl. The mixture was then centrifuged and dried by desiccation using a convection oven at 105 C for 8 hours.

After preparing the treated biomass, 0.5 L of DSMZ medium was prepared by first adding 250 mL of deionized water in a beaker. 0.65 g $(Na_4)_2SO_4$, 0.75 g KH_2PO_4, 1.45 g of $K_2HPO_4 \cdot 3H_2O$, 0.1 g $MgCl_2 \cdot 6H_2O$, 3.75 mL of $CaCl_2 \cdot 2H_2O$, 62.5 µL $FeSO_4 \cdot 7H_2O$, 1 g yeast extract, 2 g tryptone, and 0.25 g of cysteine-HCl were all then added to the beaker while stirring slowly. Once all the components were dissolved, the medium was added to bottles, which were then sealed and autoclaved.

Furfural and Phenol Inhibition on C. tyrobutyricum

In the furfural study, six different conditions each with varying concentrations of furfural were tested: 0 g/L, 0.3 g/L, 0.5 g/L, 1 g/L, 2 g/L, and 3 g/L. The bottles of each condition containing CGM medium [6] were inoculated with *C. tyrobutyricum*. Sampling was done over the course of several days. In the phenol study, the procedure used in the furfural study was repeated, however phenol was used as the inhibitor.

Analytical Methods

The concentrations of the products (butanol, butyric acid, acetic acid, and ethanol) and the substrate, glucose, were analyzed using HPLC [9]. The cell growth was analyzed by measuring the OD_{600} of the cell suspension using a spectrophotometer at a wavelength of 600 nm [9]. All fermentations conducted were done in triple.

Results

The tests were run and the optical density was measured along with the concentrations of different products. The plasmid with the ack gene knocked out is designed to increase the yield of butyrate and butanol

[8]. It can be seen that with a higher optical density comes higher concentrations of products including butanol and butyrate. The cell growth rate is logarithmic function that is calculated by using equation 1:

$$cell\ growth\ rate(h^{-1}) = \frac{(optical\ density, b) - (optical\ density, a)}{(time, b) - (time, a)} \quad (1)$$

where the cell growth rate is calculated in h-1. The equation is similar to calculating the slope of a line. The cell growth rate is essentially the slope of the growth rate.

Utilization of Corn Cob Hydrolyte by C. Tyrobutyricum

Corn cob biomass was tested on *C. tyrobutyricum* in four different conditions. Condition 1 was 80% corn cob hydrolyte; condition 2 was 40% hydrolyte; condition 3 was 20% hydrolyte; and condition 4 was 0% hydrolyte. Higher amounts of corn cob hydrolyte vary in the resulting concentrations of butanol. At 80% hydrolyte, the concentration of butanol was 1.19 g/L at the end of the trial. The highest average concentration of butanol was 2.46 g/L which was seen for the trial with 40% hydrolyte The trials with 20% and 0% hydrolyte finished with average butanol concentrations of 1.99 g/L and 2.25 g/L respectively.

The optical density increased as the experiment went on until halfway through when the density decreased or remained constant. In condition 1, the optical density changed from OD_{600} 3.885 to 3.91 over the last 120 hours of the experiment. The largest change over the last 120 hours was in condition 4 where the optical density went from 5.68 at 56.25 hours to 5.07 at the end of the experiment.

Trial 1 had by far the lowest concentration of butanol despite having the most corn cob biomass. The three trials with variations in the amount of diH2O were 19% different (conditions 2, 3, and 4) whereas there was a 40% difference between the trial with no water (condition 1) and the condition with the next lowest concentration. The highest concentration was seen with equal amounts of diH2O and corn cob hydrolyte as seen by Figure 1. The lowest concentration was observed when solely corn cob hydrolyte was utilized. When only diH2O was presented to the *C. tyrobutyricum,* the concentration was higher than when only corn cob hydrolyte was presented. For the highest concentration of butanol, equal volumes of diH2O and corn cob hydrolyte will give the highest concentration. On its own, data shows diH_2O will produce higher butanol concentrations than corn cob hydrolyte.

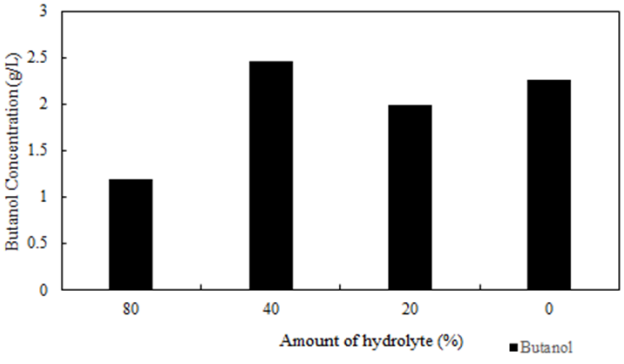

Figure 3.1. *C. tyrobutyricum* butanol concentration with various amounts of corn cob hydrolyte.

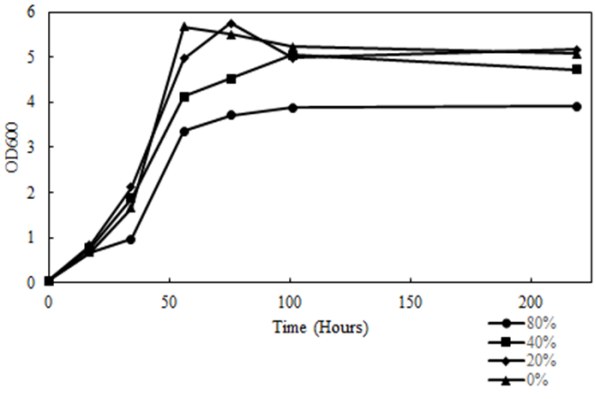

Figure 3.2. OD_{600} changes of C. tyrobutyricum with various amount of corn cob hydrolyte in the course of time

C. cellulovorans Butanol Production with varying Amounts of Glucose and Corn Cob

The *C. cellulovorans* test was run under three different conditions. The condition with 6 g/L corn cob biomass had no butyrate or butanol produced. The optical density as measured by the OD_{600} were the lowest of any of the three tests for this condition. The 10 g/L glucose and 3 g/L pretreated corn biomass condition had the most butyrate produced at a concentration of 4.95 g/L, but still no butanol was produced. The 20 g/L glucose condition produced no butanol, but still produced butyrate at a concentration of 2.60 g/L. Butyric acid was produced in this highest concentrations in the 10 g/L glucose and 3 g/L pretreated corn cob biomass condition. Butyric acid was also produced in the 20 g/L glucose condition. The 6 g/L pretreated corn cob biomass conditions resulted in no butyric acid formation. For the highest yield of butyric acid with *C. cellulovorans*, data showed corn cob biomass and glucose will be the most effective way to achieve the highest butanol titer.

As was the butyrate concentration, the optical density was the highest for the glucose and corn cob biomass cell cultures. The lowest optical density occurred for the corn cob biomass condition, similar to the butyrate production.

C. tyrobutyricum inhibition factor of phenol and furfural

The OD_{600} of each condition increased throughout the first three days of testing, but after the third day, the optical density began to decrease. The average optical density reached a peak for the 1 g/L samples on the third day. The peak was at an optical density equal to 6.13. For 2 g/L and 3 g/L, every optical density was under 0.450 indicating a lower OD_{600} value at higher concentrations of furfural.

Increasing phenol concentration is correlated with decreasing optical density. At 0 g/L, the cell growth maximized at an OD_{600} equal to 6.27 2 days after inoculation. At 2 g/L, optical density never reached an OD_{600} above 0.450 which shows phenol leads to a lower optical density.

The cell growth rate was calculated using Equation 1 which takes the optical density to find the growth rate. Figure 1 shows the changes in concentration affecting the optical density of cell cultures of *C. tyrobutyricum*. For both inhibitors, as their concentration increased, the cell growth rate decreased. The data shows the growth rate of furfural increases initially, but ultimately decreases faster than phenol. The cell growth rate, under the effect of phenol, did not change much until a concentration of 2 g/L phenol where it fell quickly. Cells with furfural experienced more cell growth at a phenol concentration, but did not experience higher cell growth at a higher concentration of inhibitor. The cell growth rate supports phenol as allowing for higher cell growth than furfural.

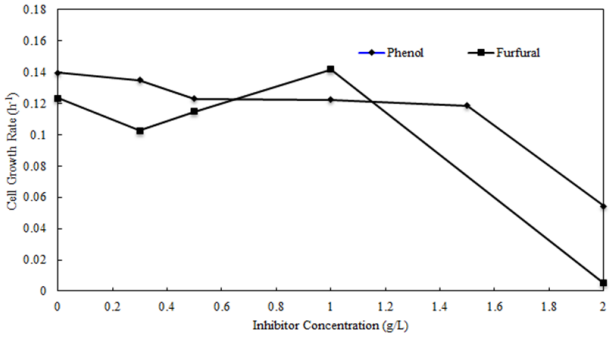

Figure 3.3. The change in cell growth as the inhibitor concentration increased by increments of 0.5 g/L. Cell growth rate is a logarithmic function

Concentrations of butanol with C. tyrobutyricum phenol and furfural

Furfural was used on *C. tyrobutyricum* to test how butyric acid and butanol production would be affected. The higher the concentration of furfural, the lower the concentration of butyric acid and butanol produced. For 2 g/L and 3 g/L of furfural, no butanol or butyric acid was produced. For 0.3 g/L furfural there was no furfural detected for the week trial. For 0.3 g/L furfural, there was 2.2 g/L butyric acid in the final product. In the 0.5 g/L and 1 g/L trial of furfural, the amount of butyric acid increased and ultimately peaked at 3.44 g/L on the last day of the 1 g/L trial. The average butanol concentrations of each trial is graphed in Figure 2.

Phenol was tested as an inhibitor with *C. tyrobutyricum* as well. The slightest amount of phenol affects the growth and production formation of this strain. The average butanol concentration for the sample with no phenol was 3.3 g/L. As the concentration of phenol increased, the amount of butanol and butyric acid decreased ultimately reaching 0 g/L of product available at 2 g/L phenol (the highest concentration of phenol tested). The amount of byproduct ethanol remained constant around 4.5 g/L, but at 1.5 g/L and 2 g/L phenol, the amount of ethanol increased. The amount of phenol increased in the product as the concentration of phenol increased in the sample. The concentration of butanol decreased as the amount of phenol increased. The amount of butanol at the end of the week can be seen in Figure 2.

The average concentration of butanol was similar at concentrations of 0 g/L and 0.3 g/L inhibitor. At 0.5 g/L of furfural, the butanol concentration decreased by only 9% whereas the concentration decreased by 29% with 0.5 g/L of phenol. The concentration of butanol did not begin to really decrease until 2 g/L furfural was introduced to the system and the concentration of butanol fell to 0. The cells with phenol produced butanol even at 2 g/L, but the concentration fell at a more gradual rate. At lower concentrations of inhibitor, data shows furfural is less inhibitory to butanol production. At higher concentrations both inhibitors will block butanol production.

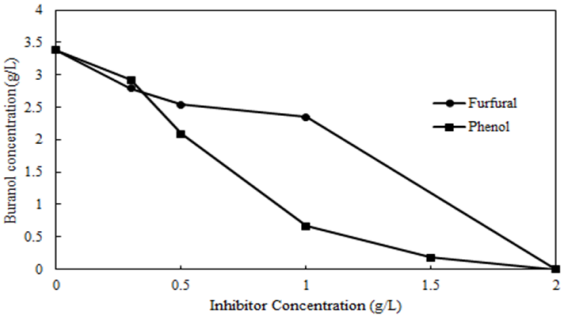

Figure 3.4. Average butanol concentration (g/L) over a period of 7 days with increasing concentrations of furfural and phenol in increments of 0.5 g/L.

Conclusion

This research analyzed the viability of corn cob biomass as a carbon source for butanol production when used in conjunction with diH_2O. C. *tyrobutyricum* produced 2.46 g/L butanol with 40% hydrolyte. *C. cellulovorans* produced 4.95 g/L butyrate with 10 g/L glucose and 3 g/L pretreated corn cob biomass in the medium. Corn cob biomass is a viable option when combined with glucose. This research also examined the effects that two inhibitors, furfural and phenol, have on the production of butanol in *C. tyrobutyricum.* Both inhibitors significantly reduced growth and production, however, they did so at different rates. At 0.5 g/L furfural, butanol production decreased by 9%, but at 0.5 g/L of phenol, production actually decreased by 29%. Production began to decrease drastically as the inhibitor concentration increased above 0.5 g/L. Various detoxification methods have the potential to further improve butanol production to decrease the cost of production.

References

[1] Baral, N., Shah, A. Microbial inhibitors: formation and effects of acetone-butanol-ethanol fermentation of lignocellulosic biomass. Appl Microbiol Biotechnol. 2014. 98:9151-9172.

[2] Cao, N.; Krishnan, J.; Gong, C.; Ho, N.; Chen, Z.; & Tsao, G. Ethanol Production from Corn Cob by the Ammonia Steeping Process using Genetically Engineered Yeast. Volume 18 No 9. 1996, p. 1013-1018.

[3] Dwidar, M., Park, J., Mitchell, R., & Sang, B. The Future of Butyric Acid in Industry. The Scientific World Journal. Volume 2012 , 10.1100/2012/471417.

[4] Ebert, "Biobutanol: the next big biofuel," Biomass Magazine, 2008.

[5] Ezeji, T., Qureshi, N., & Blascheck, H. Butanol production from agricultural residues: Impact of degradation products on Clostridium beijerinckii growth and butanol fermentation. Volume 97, Issue 6. 2007. 10.1002/bit.21373.

[6] Jones, Shawn W., et al. "Inactivation of σF in Clostridium acetobutylicum ATCC 824 blocks sporulation prior to asymmetric division and abolishes σE and σG protein expression but does not block solvent formation." Journal of Bacteriology 193.10 (2011): 2429-2440.

[7] Liu, X. Zhu Y., & Yang S. Butyric acid and hydrogen production by Clostridium tyrobutyricum ATCC 25755 and mutants. Enzyme and Microbial Technology. Volume 38. 2006, 521-28.

[8] Liu, X., Zhu, Y., & Yang, S. Construction and Characterization of ack Deleted Mutant of Clostridium tyrobutyricum for Enhanced Butyric Acid and Hydrogen Production. Biotechnol. Prog. 2006, 22, 1265−127.

[9] Ma, C., Kojima, K., Xu, N., Mobley, J., Zhou, L., Yang, S., & Liu, X. "Comparative Proteomics Analysis of High N-butanol Producing Metabolically Engineered Clostridium Tyrobutyricum." Journal of Biotechnology 193 (2015): 108-19. Comparative Proteomics Analysis of High N-butanol Producing Metabolically Engineered Clostridium Tyrobutyricum. Elsevier B.V., 5 Nov. 2014. Web. 08 Feb. 2016.

Acknowledgements

This work was supported by a research grant from the National Science Foundation (Award No. 1342390) and the Research Grants Committee (RGC) Level 2 fund (Award No. RG14657) from The University of Alabama

About the Author

Matthew Pate is a senior from Trussville, AL is majoring Chemical and Biological Engineering at the University of Alabama. He conducted his research in Dr. Margaret Liu's lab in the Department of Chemical and Biological Engineering where he has researched for a year and a half. Matthew is a member of Tau Beta Pi, an engineering honor society that honors the top engineering students in their class. He hopes to attend medical school after earning his degree this spring where he hopes to continue researching while working as a physician.

Exploring HIV Stigma in the US Virgin Islands

Elizabeth Di Valerio, Safiya George, PhD, APRN-BC

Faculty Mentor: Safiya George - sfgeorge@ua.edu
Capstone College of Nursing - The University of Alabama, Tuscaloosa, Alabama 35487

The U. S. Virgin Islands (USVI) has one of the highest HIV rates in the U.S. to date. In order to understand the high prevalence of HIV, it is important to identify the factors that contribute to HIV, especially those with relevance to the specific culture of the USVI. Quantitative surveys and qualitative in-depth interviews were conducted to examine the sociocultural factors that contribute to the high rates of HIV in the USVI. The study included a sample size of 52 participants, including community members, healthcare providers, and people living with HIV. The purpose of this secondary analysis was to identify the stigmas about HIV that persist in the USVI. Qualitative analysis of in-depth interviews using NVivo software (version 10) found that the primary stigma was being labeled as HIV-positive if an individual had been seen near an HIV-related health facility. A possible implication of HIV/AIDS-related stigmas are that they may discourage those who are HIV positive from getting treatment or disclosing their HIV status to sexual partners. These results also have implications for HIV prevention and HIV care in the USVI and similar areas.

Introduction

The Joint United Nations Program on HIV/AIDS (UNAIDS) and the World Health Organization recognize HIV/AIDS-related stigma as a barrier to treating HIV and have identified a need for research that provides better conceptual and operational definitions of stigma and that identifies different types of HIV/AIDS-related stigmas [3,7]. Past research in the Caribbean region also identified stigma as a barrier to accessing HIV care [2]. This is particularly important since the United States Virgin Islands (USVI) is ranked as having the 3rd highest rate of people living with HIV/AIDS in the US [1]. This research explored the perceptions of HIV/AIDS-related stigma and identified the most common stigmas in the USVI.

Materials and Methods

The study protocol was approved by the University Institutional Review Board and all participants provided written informed consent prior to participating in the study. The target population was adult age residents of the USVI. To be eligible, participants had to: (1) be between the ages of 18-65 years; (2) and reside in the USVI during the previous 9 months. Individuals who were not currently residing in the USVI or did not reside in the USVI within the previous 9 months were ineligible. Participants were recruited from the community, the USVI Department of Health (DoH), and local healthcare facilities, using approved study flyers and referrals. Study flyers included a brief description of the study including the purpose, procedures, duration, potential risks and benefits, and study team contact information. The flyer also clearly indicated that there was no monetary or non-monetary compensation for participation and that participation was voluntary. Interested people living with HIV contacted project staff by telephone or in person at the DoH to learn more about the study and to indicate their interest in participating. The project's purpose, procedures, potential risks and benefits were explained over the phone or in person and oral or written consent was obtained from interested participants who met initial eligibility screening. Eligibility was determined in person or via telephone using a brief screening survey. A unique study ID number was assigned once consent had been given.

Data Collection

Questionnaires were completed on password-protected laptop computers either using computer assisted personal interview (CAPI) or audio-computer assisted personal interview (ACASI). Both CAPI and ACASI are designed using the Questionnaire Development System (QDS).

Sociodemographics

A 25-item questionnaire was used to assess information regarding each participants' age range, educational level, marital status, religious background and practices and HIV testing.

Individual Interviews

Individual interviews with participants were conducted using a semi-structured interview guide. Each interview lasted between 30-60 minutes. Interviews were conducted in person by two team members (one to ask questions and one to take notes). Interviews were conducted in a private area at an agreed upon location. Each interview was audio-recorded using a digital recorder and transcribed verbatim by project team members. Participants were asked to use a pseudonym to protect their identity on audio-recordings and transcripts. Team members reviewed transcripts for any transcription or grammatical errors.

Data Management and Analysis

The PI and trained project team members conducted the analyses using the Statistical Package for the Social Sciences (SPSS) software (IBM SPSS Statistics for Windows, Version 23.0). Alpha level was set at a $p < .05$. Descriptive statistics were conducted to describe the sample and qualitative analyses were conducted by trained project team staff using NVivo software version 10 (QSR International). Trained study staff uploaded and systematically catalogued and stored transcript data in the NVivo 10 qualitative data management and analysis software program for qualitative data analysis. Content and thematic analyses and coding were used to identify themes and sub-themes related to HIV/AIDS-related stigma in the USVI. Each transcript was analyzed as one (grouped) text using constant comparative, thematic line-by-line analysis to identify salient themes.

Once an understanding of the overall text was obtained, phrases in the text were highlighted and theme names were assigned to the text. The researcher examined this data line by line, and all-important phrases were labeled with tentative theme names. Analysis of the data included elements or categories within themes. We used a precise definition for each theme in order to enable consistent recognition of when they are present, especially because of the possibility of the theme not being explicitly mentioned by an exact name. This facilitated the development of a coding scheme or structure that was used to code concepts and themes and identify the overall relationship between the codes [5].

In the attempt to reduce bias, the coders maintained an audit trail of research activities and decisions and performed member checking by asking some participants to review a list of identified themes that were presented at the community forum in the USVI. Leaders from the department of health and an HIV specialist in the USVI were asked to review main themes and provide feedback.

In order for a theme or category to be included, it needed to meet the following criteria: (1) mentioned by 15% or more of participants; and (2) recognized as a problem by each category of participants, including: community members, healthcare providers, and people living with HIV. Using SPSS software and Excel, these categories were further analyzed identify their relative frequency.

Results and Discussion

Sample Characteristics

A description of the sample is presented in Table 1. The original sample consisted of 52 participants. Forty-three of these participants completed in-depth interviews and are the focus of this paper. Participants included community members, healthcare providers, and people living with HIV, who resided on St. Croix and St. Thomas, USVI. Participants' ages and levels of education varied.

Table 1. Demographics of Participants		%
Categories	Community Members/Leaders	55.8
	Health-care Providers	27.9
	People Living with HIV	16.3
Island	St. Thomas	48.8
	St. Croix	51.2
Gender	Female	67.4
	Male	32.6
Age	13-19	11.6
	20-24	16.3
	25-23	16.3
	35-44	16.3
	45-54	16.3
	55+	23.3
Ever had an HIV Test	No	16.3
	Yes	83.7
Level of Education	8th grade or lower	9.3
	High School	14
	Associate Degree	11.6
	Some College	20.9
	College Graduate	44.2

Table 1. Demographics of Participants

Qualitative Findings

Qualitative analysis of the in-depth interviews regarding stigma indicated that there were multiple subcategories of stigma in the USVI. Coding for stigma yielded the following eight types of HIV/AIDS -related stigmas: (1) Fear of Gossip and Labeling; (2) Fear of HIV; (3) Invincibility and Appearance; (4) Preferred Ignorance and Denial; (5) Cultural Re-

sistance to Change; (6) Sexual Expectations Based on Gender or Age; (7) Resistance to Condoms or other Contraceptive Use; and (8) Prejudice against members of the LGBTQA+ Community. The coding frequency for each stigma is presented in Figure 1 and exemplar quotes for each are presented in Table 2.

The primary stigma found was the fear of gossip in the community and labeling, which typically would occur if an individual was seen around an HIV related healthcare facility. This was related to the fear of labeled if seen around an HIV health related facility, a concern for 5% of participants. The stigma was mentioned 59 times, which is nearly twice as much as the second highest stigma. Living in a small, tight-knit community, 24 participants described how unwanted gossip was spread quickly. Because of this, some participants said that they did not seek out HIV testing because they were worried about others thinking that they had HIV, simply by being tested. Healthcare providers also mentioned this stigma as being a barrier to care, as some HIV positive patients would not receive care to avoid being seen. Due to the high prevalence of being mentioned by participants, the fear of gossip and being labeled was found to be the primary stigma in the USVI and a barrier to healthcare services for HIV.

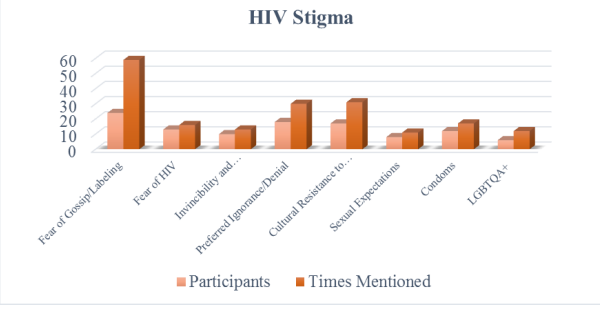

Figure 1. The number of times HIV/AIDS-related stigmas were mentioned

Fear of HIV or the fear of contracting HIV was mentioned by 13 participants, which was most correlated with a lack of education (which was analyzed using data analysis in primary research in conjunction with stigma).

Invincibility and Appearance, is based upon the idea that people who are good-looking, a certain skin color, or religious are unable to contract HIV. Some community members believe that they are "too black" to get HIV. Others are assumed to not have HIV because they are "too good-looking", or consider their religious beliefs to protect them from HIV, despite unsafe sexual practices. While being religious is not based on appearance, it did represent a factor in perceived invincibility, as some community members mentioned that their religious faith could save them from HIV, or that they believed they could cure themselves of their HIV positive status using forms of black magic.

Preferred ignorance and denial was mentioned by 18 participants as being a barrier to care. Individuals said that they would rather not know if they were infected with HIV. Healthcare providers described this stigma by many who were already found HIV positive choosing to deny their status and thereby resist care or treatments for HIV. Some participants who were HIV positive explained the stigma by saying that it was better for one to ignore their HIV-positive status to avoid being treated differently by family and friends.

The cultural resistance to change stigma is explained by the culture of the USVI being very conservative and resistant to change. This phenomenon is described by previous research as illustrated by a community readiness model, which could be utilized to assess the willingness of a community to accept change [4]. 17 participants described how the communities in the USVI were resistant to change based on long-standing cultural practices and societal norms that kept the USVI "10 years behind" other countries, as stated by one participant.

Sexual Expectations Based on Gender or Age. In the USVI there are sexual expectations, primarily for females or the elderly. Females have significantly less power as a societal norm and therefore do not have much ability or say in relationships, such as the ability to convince her sexual partner to wear a condom or be tested for HIV. Men are expected to engage in sexual activity regularly without using a condom, and doing so is an important part of the culture. The lack of female empowerment in the USVI was mentioned as being a barrier to a woman's ability to decline sexual activity, or convince her sexual partner to use a condom by many participants. The more elderly members of the population are perceived as not engaging in sexual activity, and therefore there is less outreach to get such members of the community tested for HIV as was described by several elderly members of the community. These sexual expectations are embedded in the culture and may be culturally specific to the USVI.

Resistance to Condoms or other Contraceptive Use. The stigma against condom use was described as being a barrier to safe sex by 12 participants. Younger members of society stated that they did not feel comfortable going out and buying condoms, and it was a common perception that sexual

activity "does not feel as good with one". Unprotected sexual activity is widely accepted among members of a younger generation, and the lack of female power in sexual relationships was seen as typically resulting in a woman being unable to convince her partner to use a condom.

Prejudice against Members of the LGBTQA+ Community. Members of the LGBTQA+ community are not accepted and therefore often hide their sexual orientation, making it hard for those who engage in risky sexual behaviors to be identified and treated. Individuals who are not heterosexual may live a "double life" and be married to a partner of the opposite sex, as well as engage in sexual activity with other partners that are hidden from their spouse, which is often risky sexual behavior. This may put themselves and their domestic partner (spouse) who believes he/she is engaging in safe sexual activity at risk for HIV. Because sexual orientation considered deviant in the USVI is hidden, there is an additional barrier for healthcare providers who do not know which members of the population to reach out to in order to give proper education and healthcare services to those who are not heterosexual. (See the last page of the article for Example Quotes).

Conclusion

Several different categories of stigma were identified through secondary data analysis. As shown, the most prevalent stigma was the fear of gossip and being labeled by the community. The possible implication of this stigma is that community members may choose not to pursue care in order to avoid stigma, which was described by several participants in this study. In order to counteract this stigma, increased medical confidentiality in the USVI could reduce the fear of gossip among the community.

The results of this study show that the stigma surrounding HIV is not limited to one overarching stigma. The implications of there being several different stigmas as found in this study could mean that a variety of tactics to reduce or eliminate these stigmas would be needed in the USVI and in similar populations. The findings of this study further aid current research on stigma by providing a more in-depth analysis of the concept within a culture that has a relatively high rate of HIV per capita, which may help with the creation of HIV treatment and education that can target the different stigmas within the USVI or other communities in the future.

Limitations of this study include that not all participants who completed the survey also completed the in-depth interview. Another limitation is that the community members primarily consisted of young adults, therefore certain stigmas could be more prevalent in the older community members (for example, the socially accepted prejudice against LGBTQA+ members could be present in a different proportion or strength in the older population than the primarily younger population studied). Cultural resistance to change could be another stigma affected by the age discrepancy in the study to the actual population. Certain stigmas may also have prevented some members from discussing their sexual activity, opinions, or answering questions truthfully. Because the research only studied the USVI, stigmas (especially those based on culture) may not be applicable or generalizable to other populations. Members were primarily African-American (as is the population of the USVI) so the results may differ among those of other ethnicities in other countries.

References

[1] Centers for Disease Control and Prevention. (2014). HIV Surveillance Report, 2012: vol. 24.

[2] Inciardi JA, Syvertsen JL, & Surratt HL (2005). HIV/AIDS in the Caribbean Basin. Aids Care, 17(S1), 9-25.

[3] Joint United Nations Programme on HIV/AIDS. (2007). Reducing HIV stigma and discrimination: A critical part of national AIDS programmes A resource for national stakeholders in the HIV response.

[4] McCoy HV, Malow R, Edwards RW, Thurland A, & Rosenberg R (2007). A strategy for improving community effectiveness of HIV/AIDS intervention design: The Community Readiness Model in the Caribbean. Substance use & misuse, 42(10), 1579-1592.

[5] Rubin, H. J., & Rubin, I. S. (2011). Qualitative interviewing: The art of hearing data. Sage.

[6] Virgin Islands Department of Health. (2014). HIV Surveillance 2014 Annual Data Report.

[7] World Health Organization. (2009). HIV testing, treatment and prevention: Generic tools for operational research. conference in San Juan, Puerto Rico, and the NanoBio Summit.

Appendix

Table 2. Themes and Example Quotes

Category	Example Quotes
Fear of Gossip and Labeling	"A lot of time people don't want to walk into HOPE's, uh, facility because they know that it's testing for HIV and it's in an area where anybody could see you go through the door." (Healthcare Provider) "We need something more mobile, where people could really feel more secure about their information. Because from the time you walk into the clinic, everybody's assuming you have some kind of STD or something like that." (Person Living with HIV)
Fear of HIV	"I think because so many people are just afraid of the disease that they don't want to even talk about it." (Community Member, Female) "Um…I feel like the people in the community need to take…like find out about HIV and like not be afraid to talk about it. Because I think like they're afraid to talk about it." (Community Member, Female)
Invincibility and Appearance	"People are too afraid or too proud to get tested and know their status and they judge people on looks, like "Ooh! She's hot! She probably doesn't have anything." (Community Member, Male) "Yeah. And um… I've heard people say, 'Oh I'm too black I can't get it,' and then they're positive. " (Healthcare Provider, Female)
Preferred Ignorance and Denial	"I can say all the ways of contacting people, and it's like certain people don't want to know their status because it's a kind of scary thing, to know that you have HIV" (Person Living with HIV) "People are afraid to get tested because, because they don't want to know. Um. People feel that it just couldn't happen to them, and I think a big problem here is denial. " (Community Member, Male)
Cultural Resistance to Change	"Um, lack of resources because we tend to be, I would say, ten years behind. Um, any kind of research or um, implementation of uh new measures. It's a very hard culture…in reference to change; they don't adapt quickly, like that *(audible snapping)* to change. " (Healthcare Provider, Female) "And um, I come from the perspective of protecting our culture and the environment um, and at the same time being open to change. Um, which we're not at the moment. I think our culture is very important because there are some value systems that we have in place that I don't find on the mainland that I think is beneficial to our, um, our sense of community and growth. " (Healthcare Provider, Female)
Sexual Expectations Based on Gender or Age	"Um, women don't have a lot of power here, and often end up in relationships for economic reasons, or sugar daddy kind of relationships, or, you know, I know numbers of women who get food, you know, bags of food come in and that's the exchange that she makes" (Healthcare Provider, Female) "And, uh, that people practice unsafe sex because many women in this community feel that getting pregnant is a good way to honor or keep a man. " (Community Member, Male)
Resistance to Condoms or other Contraceptive Use	"There's still a lot of um cultural prohibitions around condom use for example, around being honest about our sexual practices including you know multiple partners and um so on." (Healthcare Provider, Female) "Umm...A lot of people think condoms interfere with the feeling or the pleasure of sex. Umm...Other people, they think it ruins the mood of the moment. Some people just, you know, like I said before, they're afraid to be seen...umm...picking them up in the store or at the clinic or whatever. So they don't pick them up. Umm...Maybe they're pressured into not using them. Maybe their partner pressures them into not using them or their friends tell them, you know, it feels better without using one so they listen to other people. "(Community Member, Male)
Prejudice against members of the LGBTQA+ Community	"Like I told you before, the MSM population that are still in the closet. They, they're not coming out because they might either get killed, or get shunned from the family and what not. They are being judged and what not. So they're going to keep it to themselves and don't tell their partners. " (Healthcare Provider) "Um… it's not very progressive about homosexuality. Do you guys know what the word is for a gay man here? "Anti-man". Not like "aunty" but like "anti-man". And kids call each other that on the playground. Um… so there's like, um… a lot of, you know, this is an island that has already come even close to it having large campaigns to prohibit gay marriage here. It's a very anti-gay place. So that's hard for young men who are gay here, um… and I think gay teenagers are having a difficult time with that, because I know of two of them who are HIV-infected and are having trouble negotiating and feeling like they have any power." (Healthcare Provider, Female)

Evolutionary Optimization of Aircraft Landing Gears

Robert Ramsey [1]

1Department of Aerospace Engineering and Mechanics, The University of Alabama, Tuscaloosa, Alabama 35487

Landing gears (the undercarriage supporting the aircraft) during their lifetime, have to meet a multitude of landing and ground handling design loads whose magnitudes are several times the gross weight of the aircraft. There are many different designs for landing gears; not all of them are optimized with the best dimensions for their configuration. Also, one of the main criteria for the design is the weight of the landing gear, as an inefficient design can add unnecessary weight to the aircraft, and consequently reduce the payload or useful load. Hence, to increase the efficiency of the design and reduce the operational cost, structural optimization techniques are employed for an optimum design of landing gears.

Landing gear optimization technique involves optimizing the objective functions such as the length, width, material, slip angle, caster length etc., of landing gears for the designed loads range. In this paper, the history and explanation of evolutionary based genetic algorithms are discussed. Genetic algorithms are used to optimize the slip angle, caster length of the nose landing gear and to find the best configuration for minimizing the resistive torque generated on it. These optimized parameters for the best landing gear configuration are further analyzed and tested using finite element methods for structural stability.

Nomenclature

M_{zNW} Moment about the Z-axis
$C_{M\alpha}$ Moment Coefficient
α_g Limit angle of tire moment
$\boldsymbol{\alpha}$ Angle of Attack during landing
F_z Vertical Load
T_r Resistive torque at the ground/wheel interface
e Caster Length
β_{NW} Slips Angle (Rad)
F_{yNW} Tire lateral forces on the nose wheel
F_Y Force on the Y axis
F_N Force on the normal axis of the nose landing gear
θ_W Wheel Angle (Rad)

Introduction

Funding in any type of research usually is the reason for limitations. It is a long process to develop a possible solution for a specific problem at hand. The process of finding different solution variations alone is immensly time consuming. After that, the researcher has to hire testing groups to study how well each solution or method works. It is clearly becoming inefficient to use different variations in the experiment for research the old fashion way. Genetic Algorithms are a solution that can help cut the limitations and efficiency problems in today's complex problems.

Evolutionary Optimization Method

Genetic algorithms are a great way to cut down the cost and time needed to create solutions for real world problems. "Genetic Algorithms are a family of computational models inspired by evolution. These Algorithms encode a potential solution to a specific problem on a simple chromosome-like data structure and apply recombination operators to these structures so as to preserve critical information"[3]. In other words, genetic algorithms are a way that a computer can use evolutionary methods to determine the best possible solution for a multitude of problems.

Genetic Algorithms can take many different forms. The classical Genetic Algorithm is called a Canonical; these types of algorithms each have a set of strings called chromosomes. In each string a candidate solution is encoded. Every candidate solution has unique variables called the solutions genes.

One possible way in which the variables of a chromosome can be expressed is through binary, meaning that each bit position is recorded as either a zero or one. In Figure 1 below, "1100100111" is an example of a chromosome string expressed in binary. In this example, the one to three bit position or "110" is the material used, bit four to five or "01" is the thickness of the design, bit six or "0" is the fastener type and so on.

Each string has a fitness level which rates how well the certain gene configuration solves the problem it is given. The fitness level then determines how the search continues to find the best possible solution. The algorithms will find correlations between the strings given and the problem at hand. The three

ways algorithms generate different chromosomes are through selection, crossover, and mutation. Genetic algorithms are effective because they use these three search methods simultaneously. This is how genetic algorithms differ from other generic numerical methods. By using these three methods simultaneously, the genetic algorithm can always discover the global maximum or minimum, unlike other numerical methods. Selection is the pairing of parent chromosomes with similar fitness ranking, mimicking mate selection in genetic evolution. Two parent chromosomes then "mate" or combine, producing a new generation of strings that contain a mixture of data from both parents; this is called crossover. Goodman explains crossover as "Classical Crossover operates on two parent chromosomes" [2] and "produces one or two children or offspring"[2].There can be one or two point cross overs. If parent one and two have strings "1111111111" and "0000000000" respectively. An example on a one point cross over would be "1111000000" and a two point crossover would be "0011111000" as shown below in Figure 2.

A Chromosome or string could read 1100100111	A string could be binary or permutation
Bit position	Possible Meaning
1-3	Material used: Steel, Aluminum, wood
4-5	Thickness
6	Fastener
7-8	Stuffing
9	Corner reinforcement
10	Grip: Rubber, plastic

Figure 1. Example of Genetic Algorithm String

Lastly, mutation is the wildcard factor that happens during the cross over. The chromosome generates a gene that neither parent string has. Only one bit can mutate during a crossover and every bit has the same probability of mutation. Allowing all these search types to work at the same time makes it easy for the algorithm to find patterns in the data given to optimize their solution.

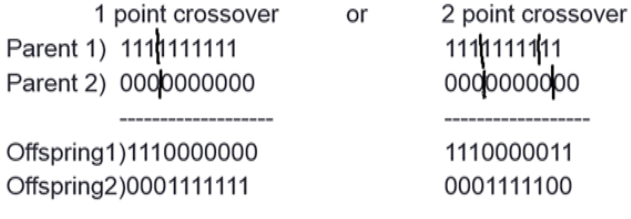

Figure 2. Visual of a one and two point crossover

Materials and Methods

Landing gear optimization involves optimizing the objective functions such as the length, width, material, slip angle, caster length etc., of landing gears for the designed load range. In this study, evolutionary optimization based Genetic Algorithms are used to optimize the slip angle, caster length of the nose landing gear and to find the best configuration for minimizing the resistive torque generated. As shown in Figure 4 the slip angle, β_{NW}, is the angle between a rolling wheel's actual direction of travel and the direction towards which it is pointing. While the caster length, e, is the horizontal length from the strut of the landing gear to the center of the nose wheel. It is important to optimize these values to minimize the resistive torque of the landing gear so the maximum amount of weight allotted for the design increases. These optimized parameters for the best landing gear configuration are further analyzed and tested using finite element methods for structural stability.

The resistive torque (T_r), for the nose wheel landing gear of one tire, at the ground to wheel interface is formulated as shown in equation 1. The resistive torque is a function of the caster length, slip angle, moment of the Z axis, and the Force of the y axis. For this studies sake, the objective functions being caster length and slip angle are left untouched for the Genetic algorithm to computationally optimize. The moment about the Z axis is formulated in equation 2, where the where the Cmα, α, and α_g are givens that the study used from references 1 and 2, the F_z is the weight of the aircraft which is also given. The generic moment equation M = F ·D is used to solve for the lateral force on the nose wheel as shown in the equation 3.

$$T_r = 2\,M_{ZNW}(\beta_{NW}) - 2e\,F_{yNW}(\beta_{NW}) \quad (1)$$

$$M_{zNW} = \left(C_{M\propto}\frac{\alpha_g}{180}sin\left(\frac{180}{\alpha_g}\propto\right)\right)F_z \quad (2)$$

$$F_Y = {M_{ZNW}}/{cos(\beta_{NW})\ e} \quad (3)$$

Matlab's Genetic Algorithms toolbox is then utilized to find the objective functions using the equations above. In the tool box the objective functions had a 30% above and below the given values as the upper and lower boundaries respectively. The values are then generated with the mutation levels of .01, .05, and .10. This means that every gene in the chromosome has a 1, 5 and 10 percent chance of mutation. I also find the values generated by the Guassian meth-

-od, which means the algorithm has no bounds and has the best solution possible. The Guassian method can be misleading, if the algorithm is not probably coded, it can possible give you results that are not physically possible.

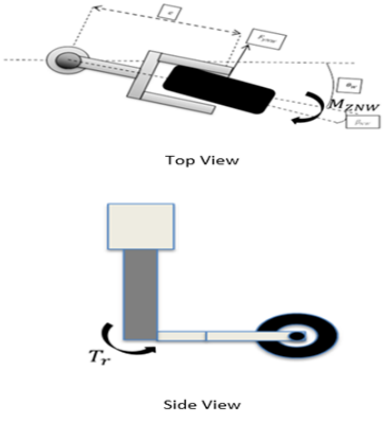

Figure 4. Nose Landing Gear Model

The finite element method is formed by use of ANSYS work bench. As shown in Figure 5.a, the top of the nose landing gear strut is fixed and not allowed to move. The Force of the Y axis is then placed at the bottom of the strut, the F_y force calculated in equation 3 along the given weight of the aircraft is used for the force in the FEM. The M_{zNW} and F_N calculated in equation 2 and 3 respectively are placed at the center of the wheel.

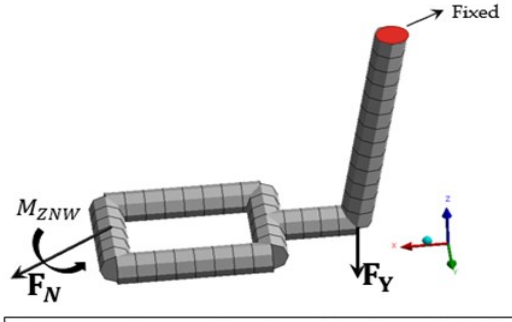

Figure 5.a: The general mesh used for the stock landing gear finite element analysis.

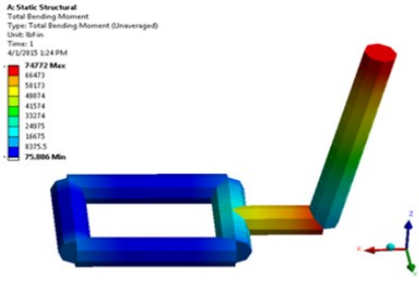

Figure 5.b: Finite Element analysis of stock landing gear.

The maximum bending moment in the stock nose landing gear is 74722 $lb_f \cdot in.$

Results

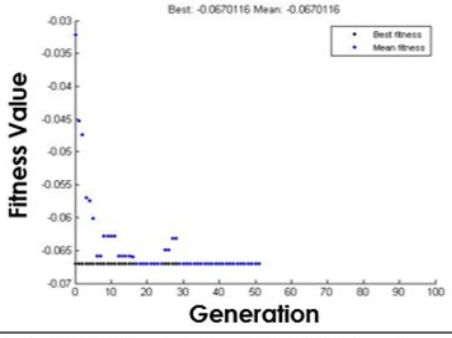

Figure 6.a: Fitness Value Vs. Generation at .01 mutation. $\beta_{NW} = 6.76°, e = .068m$

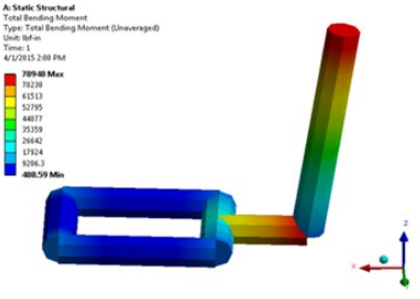

Figure 6.b: Finite Element analysis of Genetic Algorithm produced parameters at .01 mutation.

The maximum bending moment with the parameters at .01 mutation is 78943 $lb_f \cdot in.$. This is the only result in which the maximum torque was greater than the stock landing gear.

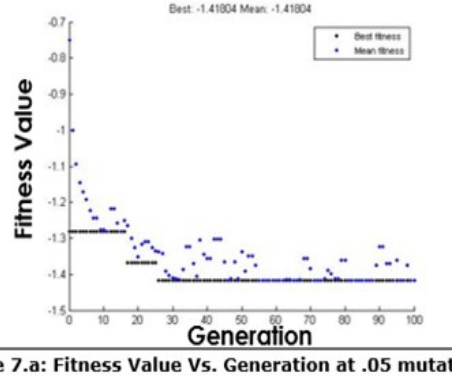

Figure 7.a: Fitness Value Vs. Generation at .05 mutation. $\beta_{NW} = 6.70°, e = .076m$

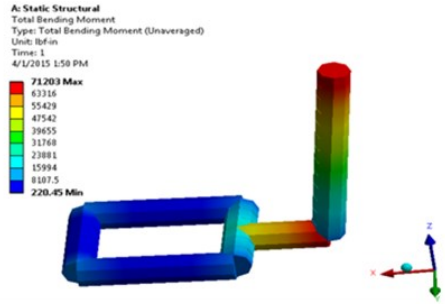

Figure 7.b: Finite Element analysis of Genetic Algorithm produced parameters at .05 mutation.

The maximum bending moment with the parameters at .05 mutation is 71203 $lb_f \cdot in.$. The bending moment was reduced by 5 percent. With the higher mutation level, it takes longer for the fitness value graph to converge.

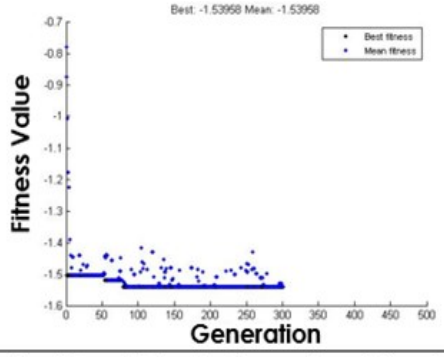

Figure 8.a: Fitness Value Vs. Generation at .1 mutation. $\beta_{NW} = 6.42°, e = .097m$

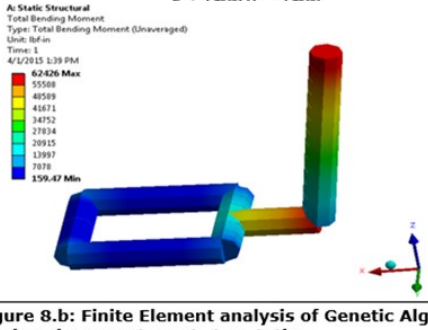

Figure 8.b: Finite Element analysis of Genetic Algorithm produced parameters at .1 mutation.

The maximum bending moment with the parameters at .1 mutation is 62426 $lbf \cdot in.$. The bending moment was reduced by 20 percent. Similar to the 5 percent mutation, the 10 percent mutation takes 300 iterations to converge.

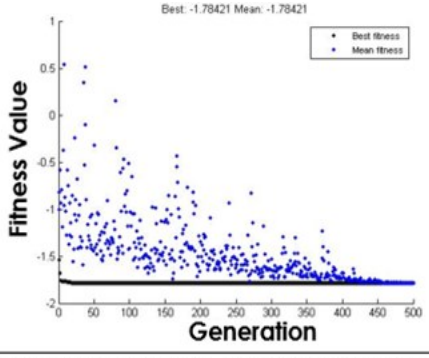

Figure 9.a: Fitness Value Vs. Generation for Gaussian mutation. $\beta_{NW} = 7.79°, e = .096m$

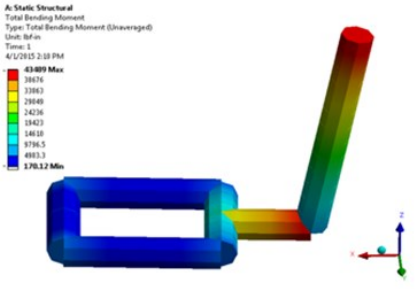

Figure 9.b: Finite Element analysis of Genetic Algorithm produced parameters for Gaussian mutation.

The maximum bending moment with the Gaussian (no bounds) parameters is 43489 $lb_f \cdot in.$. The bending moment was reduced by 42 percent. The fitness value graph took around 500 iterations to converge.

Conclusion

Three out of the four optimizations are conclusive that the resistive torque was minimized from the stock landing gear. The average amount of resistive torque reduced is 14.4% from the original 74772 $lb_f \cdot in$ with the average optimized caster length e=0.084m and slip angle =6.92°.The maximum amount of torque reduced being 41.8% with the optimal caster length e =.096m and slip angle =7.79°. The results from this study proved that generic algorithms can be utilized for innovating optimization problems.

Future Work

I hope to continue my study of genetic algorithms for my graduate research. My current interest is defense and space exploration. I would like to incorporate more complexed genetic algorithms into the research I hope to conduct.

Acknowledgments

Dr. Vinu Unnikrishnan was my mentor while conducting this research, Hasson Syed assisted in the finite element analzyation and Jessica Ramsey and Madison Stankevich assisted in revision and editing.

References

[1] Atabay, Elmas, and Ibrahim Ozkol. "Application of a magnetorheological damper modeled using the current–dependent Bouc–Wen model for shimmy suppression in a torsional nose landing gear with and without freeplay." Journal of Vibration and Control (2013): 1077546312468925.

[2] Goodman, E. (2009, June). Introduction to Genetic Algorithms. Retrieved from PDF.

[3] Whitley, D. (1994). A Genetic Algorithm Tutorial. Retrieved from PDF.

[4] “Reduced order H∞ control design of a nose landing gear steering system." Proc. of 12th IFAC Symposium on Transportation Systems, Redondo Beach, CA. 2009.

About the Author

Originally from Newark, Delaware, Robert Ramsey is currently a senior majoring in Aerospace Engineering and Mechanics with a minor in mathematics. He first began researching as a freshmen with the University of Alabama’s Emerging Scholars Program. His areas of interest include genetic algorithms for optimization of air- and space-craft systems along with space exploration. He looks to continue his education in the near future with either perusing a Masters or PhD Degree in Aerospace Engineering.

Mechanisms of Ethanol-Induced Developmental Neurotoxicity

Courtney Rentas

During synaptogenesis, the developmental stage referred to as the brain growth spurt period, inhibition of neuronal activity can be accomplished by blocking N-methyl-D-aspartate receptors (NMDA) receptors or by excessive activation of gamma-aminobutyric acid (GABA) receptors in the developing brain. Ethanol has both GABAmimetic and NMDA antagonistic properties, and thus causes apoptosis in the developing brains of many different organisms; the mechanism underlying ethanol-induced neurodegeneration provides a probable explanation for the hallmark characteristics of human fetal alcohol syndrome (FAS) and the permanent neurobehavioral side effects implicated by the disorder. Only a single instance of ethanol intoxication, lasting for a few hours, is sufficient to trigger apoptotic neurodegeneration in the developing brain. Synaptogenesis occurs at different times relative to birth in different organisms; in rats and mice it is a postnatal event, but in humans it extends from the 6th month of gestation to several years after birth. Therefore, there is a period in fetal development that extends into the first several years of life during which immature central nervous system (CNS) neurons are highly sensitive to environmental agents. Many drugs of abuse follow similar mechanisms, thus extending the application of current toxicolo-

Introduction

Prenatal exposure of the human fetus to ethanol causes a neurotoxic syndrome, known as Fetal Alcohol Syndrome (FAS) [4]. The prevalence of FAS is estimated to be approximately 1:1,000 children, equating to 40,000 new instances in the United States each year [6]. Children that suffer from FAS most notably show reduced brain mass; this results in a spectrum of neurobehavioral problems from hyperactivity to learning disabilities and major depressive disorder in adulthood [10]. Recent research has identified potential mechanisms to explain the widespread neurodegeneration and cellular devastation that results from ethanol exposure to the developing brain.

Though it has been established that ethanol induces apoptosis (cell suicide) of neurons in the developing brain during synaptogenesis to induce FAS, the mechanisms underlying the deleterious effects of ethanol remain unknown [2]. A definitive discovery in relation to the environmental influences on neurodegenerative diseases came three decades ago when Olney determined that glutamate destroys neurons in the developing brain [7]. Olney further hypothesized that during synaptogenesis, neurons with NMDA receptors are highly sensitive to both overstimulation and understimulation, triggering excitotoxic neurodegeneration and apoptosis, respectively. In vivo studies have confirmed that during synaptogenesis, abnormal increases in NMDA glutamate receptor activity leads to excitotoxic neurodegeneration, whereas the inhibition of neuronal activity induces neuronal apoptosis. Inhibition of neuronal activity can be accomplished by blocking NMDA glutamate receptors or by excessive activation of gamma-aminobutyric acid (GABA) receptors in the developing brain by GABAmimetic drugs [8].

Ethanol has both GABAmimetic and NMDA antagonist properties and thus causes apoptosis in the developing brains of many different organisms, or Fetal Alcohol Syndrome (FAS) [1, 5, 8]. Ethanol induces apoptosis by blocking NMDA glutamate receptors and excessively activates GABA receptors in the forebrain. During the period of synaptogenesis, the brain is highly vulnerable to apoptotic death and ethanol consumption can result in the death of millions of neurons, which results in FAS [2]. A greater understanding of neuronal apoptosis during synaptogenesis can therefore help to explain the diminished brain mass and neurobehavioral disturbances that are seen in patients that suffer from FAS.

Pharmacological Models of Apoptotic Neurodegeneration:

NMDAmimetics

It was determined by Ikonomidou, that when administered to 7-day-old rats, MK801- an NMDA antagonist, triggers an apoptotic response affecting neurons throughout the developing brain [3]. Further studies testing the effects of other NMDA antagonists including phencyclidine (PCP) and carboxypiperazin-4-yl-propyl-1-phosphonic acid (CPP) found a robust apoptotic

response in the developing brain of rats. The drugs were administered in doses that would keep the rats intoxicated for 8 hours, and after 24 hours the brains were analyzed for neurodegeneration via silver-staining techniques. ANOVA revealed a significant effect of the severity of brain damage, with multiple comparisons showing significant, robust increases in apoptosis at 4 hours. Following his previous work, Ikonomidou et al. (2000) devised an experiment to test whether ethanol, an NMDA glutamate receptor antagonist, would induce neuronal apoptosis in developing rats' forebrains as a means of modeling FAS [2]. Researchers administered an ethanol solution or saline solution, respectively, to the experimental and control groups of 7 day old rats undergoing synaptogenesis. The rats' forebrains were analyzed via histological staining techniques to visualize neurodegeneration. It was determined that rats injected with the ethanol solution had dense, widespread neurodegeneration whereas the rats' brains treated with saline showed minimal neurodegeneration not attributed to apoptosis. Furthermore, the neurodegenerative patterns observed in ethanol treated rats were more extensive than patterns observed in other NMDA antagonist drugs.

Further analysis of neuronal cell death was conducted in the brains of the experimental and control rats. In rats injected with saline, 0.13 to 1.55% of the total neuronal population had degenerated; the cell death is attributed to spontaneous apoptosis found naturally in developing rats' brains. However, in ethanol treated rats, 5-30% of the total neuronal population had degenerated upon analysis.

GABAmimetics

Ikonomidou found robust neurodegeneration following administration of ethanol in regions of the brain not containing NMDA receptors [2]. This prompted researchers to test the effects of various GABAmimetic in 7 day old rats. Following exposure, widespread neurodegeneration induced by neuronal apoptosis was observed, as confirmed by ultrastructural analysis via silver-staining techniques.

In a follow-up study, Young exposed 7 day old rats to one dose (40 mg/kg) of ketamine or midazolam (both GABAmimetic drugs) or a saline solution [12]. 24 hours later, caspase immunohistochemistry was used to analyze the brains of the rats exposed to the various conditions. At doses of 20 mg/kg and 30 mg/kg, ketamine showed significant ($P<0.05$ and $P<0.01$, respectively) increases in caspase-3 activity, and thus eventual neuronal apoptosis. At a dose of 40 mg/kg, there was 100% increase in caspase-3 activity ($P<0.005$).

Ethanol has NMDA antagonistic properties and functions as a GABAmimetic; various studies have demonstrated that ethanol administration induces a more robust apoptotic response than GABAmimetic drugs or NMDA antagonist drugs alone [8]. Rats exposed to ethanol, following the same methodology outlined previously in Ikonomidou's study, showed a greater degenerating cell density relative to overall cell density in all but 1 of the brain regions tested, the parietal cortex layer II [2].

Threshold of Ethanol-induced Neurotoxicity

Ikonomidou injected rats with different doses of ethanol in order to better understand the effects of ethanol on neurodegeneration [2]. The critical toxic threshold of ethanol in the blood stream was determined to be 200 mg/dl. After 4 hours at a blood level concentration of 200 mg/dl, apoptosis was induced and neurodegeneration was more observable and widespread.

In 2001, Tenkova et al. conducted experiments to identify the presence of caspase-3 following ethanol exposure [11]. 7 day old mice were injected with a 20% ethanol solution subcutaneously 2 times over the course of 2 hours in the experimental condition, and a 100% saline solution 2 times over the course of 2 hours in the control condition. Following ethanol exposure or saline exposure, the mice were anesthetized and their brains were removed and processed for capsase-3 immunohistochemistry analysis. After only 2 exposures to the ethanol solution, there was robust caspase-3 activation throughout the forebrain.

Discussion

The aforementioned results suggest several potential mechanisms of ethanol-induced neurotoxicity in the developing brain. It has been shown that ethanol functions as a GABAmimetic drug and a glutamate antagonist to induce robust neurodegeneration throughout the developing brain. The implications of the data extend beyond neurotransmission and offer a potential mechanism for the neurobehavioral and cognitive abnormalities observed in children suffering from FAS.

The Role of Glutamate antagonist and GABAmimetic Drugs in Apoptotic Neurodegeneration

Recognition of the period of neurodegenerative vulnerability is crucial in understanding the implications of drinking ethanol during pregnancy, as illustrated by children that suffer from FAS. Animal models of this vulnerable period of neural development provide researchers with the ability to identify and control the variables thought to play a role in neurodegeneration. However, interspecies differences, such as length of interspecies-equivalent developmental stages, must be identified and taken into consideration when generalizing findings. In humans, the period of vulnerability extends from the third trimester of pregnancy and into the first several years of life [3]. The equivalent period of vulnerability to apoptotic neurodegeneration in rats begins 1 day before birth and lasts 14 days after birth. Ikonomidou et al. (2000) determined that when NDMA antagonistic drugs are administered to 7 day old rats undergoing the developmental brain growth spurt, significant neurodegeneration is observed [3]. Ethanol is an NMDA antagonistic drug that causes devastating apoptotic neurodegeneration in the developing fetus when a mother consumes ethanol while pregnant. This early study on the mechanisms implicated in FAS suggested that ethanol induced neuronal apoptosis by blocking NMDA glutamate receptors like other NMDA antagonists [3]. After injecting 7 day old rats with either a saline solution or an ethanol solution, it was determined that the rats exposed to ethanol showed robust neurodegeneration unrelated to natural, spontaneous apoptotic responses in the developing brain. Furthermore, it was determined that when exposed to ethanol, the patterns of neurodegeneration were similar to the patterns of neurodegeneration observed in the brains of rats exposed to other NMDA antagonists; this finding supports the hypothesis that ethanol works as an NMDA antagonist, blocking glutamate receptors, to induce neuronal apoptosis. Whereas patterns of neurodegeneration were similar across ethanol and other NMDA antagonistic drugs like PCP and CPP, the neurodegeneration observed in rats exposed to ethanol was far more robust than the neurodegeneration observed in rats exposed to PCP or CPP. This suggests that ethanol is working by a dual mechanism to induce neurodegeneration [2].

In addition to the highly robust apoptotic response observed in the brains of rats exposed to ethanol, neurodegeneration was observed in regions of the brain lacking NMDA receptors; this finding prompted researchers to examine the role of ethanol as a GABAmimetic drug. Ethanol potentiates the effects of the neurotransmitter GABA at GABA receptors and thus acts as a GABAmimetic drug in addition to an NMDA antagonist. Other GABAmimetic drugs including pentobarbital and diazepam were determined to induce neurodegeneration in the brains of rats exposed to the drugs. This finding led researchers to hypothesize that ethanol not only functioned as an NMDA antagonist when administered to rats, but also as a GABAmimetic, leading to robust neurodegenerative effects in the developing forebrain [2].

When exposed to GABAmimetic drugs, researchers found increased caspase-3 activity in the brain. Caspase-3 is a crucial enzyme needed for apoptosis, so increased levels of caspase-3 indicate increased apoptosis and eventual neurodegeneration in the developing rat brain [9]. Since ethanol administration leads to robust neurodegeneration in the developing brain, research on other GABAmimetic drugs suggests a potential mechanism of action for ethanol; ethanol likely induces neurodegeneration via apoptosis as a positive modulator of GABA receptors throughout the brain. When exposed to ketamine, a GABAmimetic drug, caspase-3 activity increased significantly in the 7 day old rat brain; the amount of caspase-3 activity increased as the administered dose increased from 20 mg/kg to 40 mg/kg. These results indicate a positive correlation between the dose of ethanol and the level of caspase-3 activity, which ultimately leads to neurodegeneration [12].

Ikonomidou et al. (2000) added further support to the dual-mechanism hypothesis of ethanol induced neural apoptosis. When comparing regions of the brain in rats that were exposed to an NMDA antagonist drug, a GABAmimetic drug, and ethanol, which has properties of both an NMDA antagonist and GABAmimetic, the most robust neurodegeneration was observed in rats exposed to ethanol [2]. Furthermore, the study offers a potential mechanistic explanation for the devastating effects of FAS. Whereas rats exposed to only an NMDA antagonist or GABAmimetic drug show neurodegeneration, the effects of ethanol are more widespread and devastating.

The robust neuronal apoptosis in observed in

the rat brains exposed to ethanol suggest that the devastating effects of FAS in children result from the dual mechanism of action implicated by ethanol following prenatal exposure to the drug. The results from various studies suggest that ethanol functions as both an NMDA antagonist and a GABAmimetic to induce neuronal apoptosis during synaptogenesis in the developing brain. By working through a dual mechanism, ethanol induces robust neurodegeneration unable to be replicated by NMDA antagonist drugs or GABAmimetic drugs alone. The findings from these studies shed light on the devastating effects ethanol consumption has on the developing fetus, and offers insight into the permanent damage resulting from intrauterine ethanol exposure.

Threshold Conditions for Triggering Apoptosis Following Exposure to Ethanol

After exposing rats to differing doses of ethanol over varying durations of time, it was determined that the neurodegenerative effects of ethanol cannot be attributed to the dose administered alone, but rather to the rate of drug administration and the duration of time in which the blood alcohol concentration of ethanol is above the critical toxic threshold of 200 mg/dl. This finding is important as it describes a common misconception regarding the amount of alcohol consumption necessary to induce FAS in the developing fetus. Ikonomidou et al. (2000) suggest that the effects of ethanol are independent of the amount consumed, but instead depend on the blood alcohol concentration of ethanol. The study suggests that 200 mg/dl of ethanol is the critical toxic threshold for inducing neuronal apoptosis in the developing brain, and the duration of time in which the blood alcohol concentration is above 200 mg/dl is indicative of whether or not neurodegeneration will be observed. The results indicate that after 4 hours of prolonged exposure to ethanol with a blood alcohol concentration of 200 mg/dl, neurodegeneration in the developing brain is widespread and detrimental. This has important implications for expecting mothers who consume ethanolic beverages, as the study suggests that one night of drinking can potentially lead to FAS in the developing fetus. It would take about three standard drinks per hour for two and a half consecutive hours for a 140 pound woman to reach a BAC of 0.20%, which is equivalent to a blood alcohol concentration of 200 mg/dl.

Following the work of Ikonomidou, Tenkova determined that caspase-3 activity was present as early as 2 to 3 hours after ethanol activity at a blood concentration level of 200 mg/dl [11]. As caspase-3 activity is indicative of apoptosis, these finding suggest that after only 2 to 3 hours after ethanol exposure at blood concentration levels of 200 mg/dl, neuronal apoptosis can occur. This study supports previous studies which suggest that the effects of ethanol on the developing brain are rapid and detrimental, as only one incident of ethanol intoxication is necessary to induce apoptosis of millions of neurons in the developing brain. Though model organisms were used in the research methodology, the applications of this study extend to pregnant women that consume ethanol. FAS occurs as a result of prenatal exposure to ethanol, and prior to these studies, the amount and duration of ethanol exposure required to induce FAS was drastically underestimated. This particular finding suggests that one incident of ethanol intoxication is sufficient to cause millions of neurons in the developing brain to commit cell-directed suicide, which is progressive and permanent [11].

The neurobehavioral disturbances that result from FAS are the most debilitating effects of ethanol on the developing brain [8]. While there are several potential mechanisms implicated in the widespread neurodegeneration observed in the brains' of those that suffer from FAS, ethanol's ability to induce apoptotic neuronal cell death during synaptogenesis is likely the cause of the decrease in brain mass associated with FAS. The neurobehavioral disturbances associated with decreased brain mass, including ADHD, psychotic disorders and major depressive disorder later in life, are likely a result of the widespread neuronal apoptosis that ethanol induces throughout the brain, most significantly in the forebrain region [8]. The conclusion that ethanol induces neuronal apoptosis by interfering with glutamatergic neurotransmission at NMDA receptors and GABAergic neurotransmission via positive modulation at GABA receptors, aids in clarifying the neurobehavioral implications of FAS.

Extended Application of Findings

Though FAS is the most significant implication of neurotoxicity induced from ethanol consumption, there are other disorders known to arise from ethanol administration as well. Depending on when ethanol is administered during synaptogenesis, early, middle, or late in the process, different patterns of neuronal apoptosis are observed in the developing brain. The various

patterns of neurodegeneration give rise to different neurobehavioral problems including ADHD and psychotic disorders [8]. Though it is believed that many psychiatric disorders have a genetic component to heritability, environmental factors may influence onset of the disorder. Prenatal exposure to ethanol is currently considered an environmental factor that may induce psychiatric disorders in children and adults later in life, offering another example of the neurotoxic devastation induced by ethanol.

Though ethanol is the most commonly abused drug, other drugs are abused by expectant mothers and can cause permanent, damaging effects in the developing fetus via similar mechanisms to ethanol-induced neuronal apoptosis. Drugs tested in previous experiments that serve as GABAmimetics like diazepam and NMDA antagonist drugs like ketamine can cause widespread neuronal apoptosis in the developing brain [8]. Understanding the mechanisms involved in neuronal apoptosis along with definitive research demonstrating the progressive devastation intrauterine exposure to GABAmimetic drugs and NMDA antagonistic drugs cause may lead to a lower prevalence of such disorders in the future. Better education about the potential effects of drug usage in expectant mothers may effectively combat the prevalence of disorders that are preventable by abstaining from drug usage during pregnancy [8].

Another important recent discovery is that many anesthetics administered in children serve as GABAmimetic drugs or NMDA antagonists [8]. Various doses of "anesthetic cocktails" comprised of ketamine, nitrous oxide, and various benzodiazepines are administered to render the child unconscious and resistant to pain for the course of the surgery; future research in the field is aimed at uncovering whether blocking NMDA receptors and GABA receptors for extensive periods of time in children is analogous to exposing the developing brain to ethanol for hours at a time. Since a single episode of ethanol intoxication is sufficient enough to induce neuronal apoptosis in the developing brain, research is currently aimed at testing the impact of pediatric anesthetics on the brains of children exposed to anesthetics for prolonged periods of time during surgery [8]. Though no research has been conducted in humans on this topic, recent research has found that when nitrous oxide and midazolam, typical GABAmimetic anesthetics, were administered in rats, irreversible neuronal

References

[1] Harris RA, Proctor WR, McQuilkin SR, Klein RL, Mascia MP, Whatley V, Whiting PJ, & Dunwiddie TV. (1995). Ethanol increases GABAA responses in cells stably transfected with receptor subunits. Alcohol Clinical Experimental Research, 19: 226–232.

[2] Ikonomidou C, Bittigau P, Ishimaru MJ, Wozniak DF, Koch C, Genz K, ... & Olney JW. (2000). Ethanol-induced apoptotic neurodegeneration and fetal alcohol syndrome. Science, 287(5455): 1056-1060.

[3] Ikonomidou C, Bosch F, Miksa M, Bittigau P, Vöckler J, Dikranian K, ... & Olney, JW. (1999). Blockade of NMDA receptors and apoptotic neurodegeneration in the developing brain. Science, 283(5398): 70-74.

[4] Jones KL & Smith DW. (1975). The fetal alcohol syndrome. Teratology, 12(1): 1-10.

Jevtovic-Todorovic V, Wozniak DF, Benshoff N & Olney JW. (2001). Commonly used anesthesia protocol causes neuronal suicide in the immature rat brain. Society of Neuroscience Abstract, 27:772.4.

[5] Lovinger DM, White G, Weight FF (1989). Ethanol inhibits NMDA activated ion current in hippocampal neurons. Science, 243: 1721–1724.

[6] May PA, & Gossage JP. (2001). Estimating the prevalence of fetal alcohol syndrome: A summary. Alcohol Research and Health, 25(3): 159-167.

[7] Olney JW. (1969). Brain lesions, obesity, and other disturbances in mice treated with monosodium glutamate. Science, 164(3880): 719-721.

[8] Olney JW. (2002). New insights and new issues in developmental neurotoxicology. Neurotoxicology, 23(6): 659-668.

[9] Porter AG & Jänicke RU. (1999). Emerging roles of caspase-3 in apoptosis. Cell death and differentiation, 6(2): 99-104.

[10] Streissguth AP, Bookstein FL, Barr HM, Sampson PD, O'Malley K & Young JK. (2004). Risk factors for adverse life outcomes in fetal alcohol syndrome and fetal alcohol effects. Journal of Developmental & Behavioral Pediatrics, 25(4): 228-238.

[11] Tenkova T, Muglia L, Dikranian K, Roth KA

& Olney JW. (2001). Ethanol triggers a widespread pattern of caspase-3 activation and an identical pattern of apoptotic neurodegeneration in the developing mouse brain. Society for Neuroscience, 27: 450.

[12] Young C, Jevtovic□Todorovic V, Qin, YQ, Tenkova T, Wang H, Labruyere J & Olney JW. (2005). Potential of ketamine and midazolam, individually or in combination, to induce apoptotic neurodegeneration in the infant mouse brain. British journal of pharmacology, 146(2): 189-197.

A Study of the Role of Music and Religion on African American Adolescent Females' Sexual Beliefs and Behaviors

Makenzie Plyman, Safiya G. Dalmida

Faculty Sponsor: Safiya George Dalmida sfgeorge@ua.edu
Capstone College of Nursing , The University of Alabama, Tuscaloosa, AL, 35487

African Americans (AA) have the highest rates of HIV/AIDS among any U.S. racial or ethnic group. The literature revealed that support from religious programs has greater impact than religion itself, and music negatively effects images of self-worth. However, previous studies did not focus solely on AA adolescent girls and did not examine the effects of different types of religion and types of music beyond rap and hip hop. Considering the significant involvement and influence of religion in AA youth and the excess of sexual imagery in music videos (in 47% to 76% of videos), the objectives of the secondary analysis are to determine the role of music and religion in the sexual decision making and behaviors of AA adolescent females. The original study used focus groups, qualitative methods, and computerized questionnaires to identify cultural factors that influence sexual behaviors and decision making. The sample size consisted of 32 AA adolescent females 15 to 19 years old who were recruited from a high school and several YMCAs. More than half (66%) of the females were sexually active. NVivo version 10 and SPSS software version 23 were used to determine the importance of religion and music preference on the sexual decision making and behaviors of AA adolescent girls. The findings could help to highlight the role of these factors in AA adolescent girls' sexual beliefs and behaviors, as well as help to inform people who work with AA adolescent females so as to create more effective intervention programs.

Introduction

African Americans (AA), specifically adolescent females, have the highest rates of human immunodeficiency virus (HIV) and acquired immunodeficiency syndrome (AIDS) among any U.S. racial or ethnic group [2] (see Figure 1). With the average youth listening to music 1.5 to 2.5 hours per day [7] and an average of 31 hours weekly [10], music's influence seem to be very threatening, particularly if the lyrics are negative [4, 7]. Studies have reported an excess of sexual imagery in music videos (in 47% to 76% of videos) [12]. Additionally, churches' norms currently do not provide very open settings where young people can talk with faith leaders about sex, relationships, sexually transmitted infections (STIs) and HIV/AIDS [5]. Considering the significant involvement and influence of religion in AA youth and their exposure to sexually explicit music, the objectives of this secondary analysis were to determine the role of music and religion in the sexual decision making and behaviors of AA adolescent females. The literature revealed that support from religious programs has greater impact than religion itself, and music negatively affects images of self-worth [8, 12]. Previous studies, however, did not focus solely on AA adolescent girls and did not examine the effects of different types of religion or music beyond rap and hip hop [1, 5, 7-10, 12].

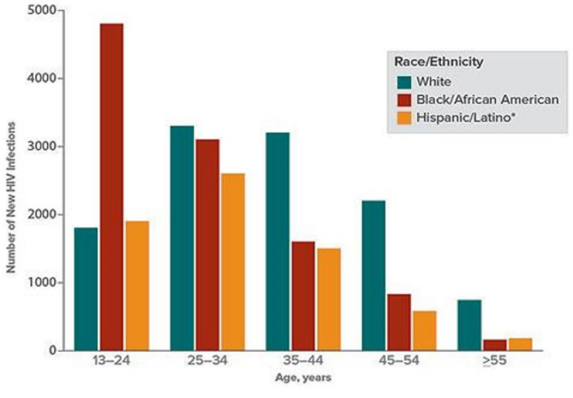

Figure 1. Number of New HIV Infections by Age and Race/Ethnicity

The original study used focus groups, interviews, qualitative methods, and computerized questionnaires to identify cultural factors that influence sexual behaviors and decision making. The sample size consisted of 32 AA adolescent females (15 to 19 years old) from a high school and several YMCAs. More than half (65.6%) of the females were sexually active. Next steps include using NVivo and SPSS software to determine the importance of music preference and religion on the sexual decision making and behaviors of AA adolescent girls.

Materials and Methods

The original study used focus group interviews, qualitative methods, and computerized questionnaires to identify cultural factors that influence sexual behaviors and decision making among 32 AA adolescent females ages 15 to 19 years old. Participants were recruited from two high schools and several YMCAs using study flyers. The study protocol was approved by the University Institutional Review Board and each participant provided written informed consent or assent with parent/guardian consent prior to participating in the study. Eligible participants had to: 1) provide assent or consent; 2) provide parental consent (if child < 18 years old); 3) identify as Black or AA; 4) be 15 to 19 years old; (5) be female by birth and 6) have already had their first menstrual period (so that participants were in a similar stage of pubertal development). The girls were compensated $40 for their time spent participating in the study.

Focus Groups

Girls participated in one of three separate focus groups, each of which consisted of approximately 10 to 12 girls. Groups were facilitated by the PI and a trained, AA female research staff, using a script/guide [6]. Only pseudonyms were used. Each focus group lasted 60 to 90 minutes and was audio-taped and then transcribed verbatim. Participants were asked to discuss the role that social factors or cultural experiences, beliefs, values and practices might play in young females' decisions about sex and sexual behavior, if any. If music or media was not spontaneously discussed, the following probes were used, "What role, if any, do you think music, movies, other media, or the internet might play? And how, why or why not?" and "What role if any does religion or your religious or spirituality beliefs play? How, why, or why not?".

Computerized Data Collection

Participants used laptop computers to complete questionnaires using the audio computer assisted self-interview (ACASI) software of the Questionnaire Development System. The surveys and questionnaires included a socio-demographic questionnaire and the AIDS Risk Behavior Assessment (ARBA).

Sociodemographics.

Each participant completed a brief sociodemographic form, which assessed age, highest grade completed, parental income, employment status, living arrangements, number of children etc.

Sexual Behavior. The adolescent version of the AIDS Risk Behavior Assessment (ARBA) was used to assess sexual history and practices [4]. The ARBA is a structured interview with 45 main questions, with subquestions, designed specifically for use with adolescents to assess their self-reported behaviors associated with HIV-infection and uses a skip structure so that initial screening questions answered in the negative are not followed by more detailed items [4]. The ARBA assessed sexual behavior (e.g., lifetime sexual intercourse, frequency, contraceptive use, high-risk sexual behavior) within the past 30 days and the past 3 and 6 months. The ARBA has been found to be reliable, with reported alpha coefficients greater than .70, in samples of predominantly AA adolescents [4]. The ARBA has no total score or subscale scores.

Data Analysis

NVivo and SPSS software were used to determine the role of music and religion on the sexual decision making and behaviors of AA adolescent girls.

Qualitative Data Analysis.

NVivo software version 10 for qualitative analysis (QSR International) was used to analyze narrative data from focus group transcripts and to examine coding/nodes in order to determine frequency of coding references to religion and music. Transcripts were analyzed using content analysis. Comparisons were then made across focus groups. Once an understanding of overall text was obtained by reading transcripts and data several times, phrases in the text were highlighted and theme names were assigned to the text, as they emerged from the narratives. Line-by-line coding and thematic analysis was done and all important phrases were labeled with tentative theme names [3]. A coding scheme was developed, using a precise definition for each theme, and was used to code concepts and themes and identify the overall relationship between the codes [11]. Three team members reviewed the coding scheme and transcripts, then the initial coding scheme was modified by merging some of the coding categories that were similar. All of the transcripts were recoded with the revised coding scheme, which yielded non-overlapping themes. Percent agreement was greater than 80% on all codes. To check credibility of the data, member checking was done by summarizing the main themes discussed at the end of each group asking the participants if the summary reflected the discussion. All participants agreed that the themes were consistent with what was discussed.

Quantitative Analysis.

Descriptive statistics including frequencies percentages from the demographic data and mean ages

were calculated using SPSS 23.0 statistical software package. Crosstabs and Chi square tests were also conducted to examine associations among factors.

Results

The sample included thirty-two AA girls ages 15 to 19. More than half (66%) of the females were sexually active. The average age for having vaginal sex for the first time was 15.68 (±1.60) years. Sixteen percent (n=5) never attended religious services, 56% (n=18) attended monthly, 25% (n=8) attended weekly, and 3% (n=1) attended daily. Of those who never attended religious services, all five were in the high sexual risk behavior (SRB) category. Of those who attended religious services monthly, six had low SRB, and 12 had high SRB. Of those who attended religious services weekly, one had low SRB, and seven had high SRB. This relationship was found to be significant, with a p value of 0.045 (see Figure 2). Nineteen percent (n=6) were not associated with a church or temple. Of those who never attended religious services, five had had vaginal sex before. Of those who attended religious services monthly, five had never had vaginal sex, and 12 had. For those who attended religious services weekly, one girl had never had vaginal sex, and seven had. For those who attended religious services daily, one had had vaginal sex. Seventy-eight percent (n=25) identified themselves as Christian or Baptist. Of those who were not associated with a church or temple, two had low SRB, and four had high SRB. Of those who identified as Christian or Baptist, four had low SRB, and 20 had high SRB (see Figure 3). For those who identified as Christian or Baptist, four had never had vaginal sex before, and 21 had. For those who were not associated with a church or temple, two had never had vaginal sex before, and four reported a history of vaginal sex.

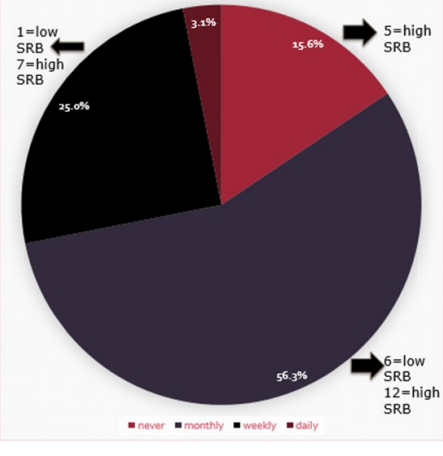

Figure 2. Relationship between Religious Attendance and SRB

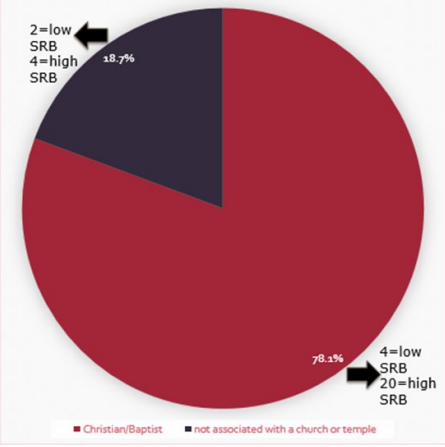

Figure 3. Relationship between Religious Affiliation and SRB

Forty-four percent (n=14) reported getting their information about HIV/AIDS from the TV or radio. Of those who received their information about HIV/AIDS from the TV or radio, four were in the low sexual risk behavior (SRB) category, and nine had high SRB. For the remaining participants who did not get information about HIV/AIDS from the TV or radio, three had low SRB, and 15 had high SRB (see Figure 4). For those who obtained their information about HIV/AIDS from the TV or radio, four had never had vaginal sex, and 10 had. For the remaining participants who did not get information about HIV/AIDS from the TV or radio, 15 reported a history of vaginal sex and three had never had vaginal sex.

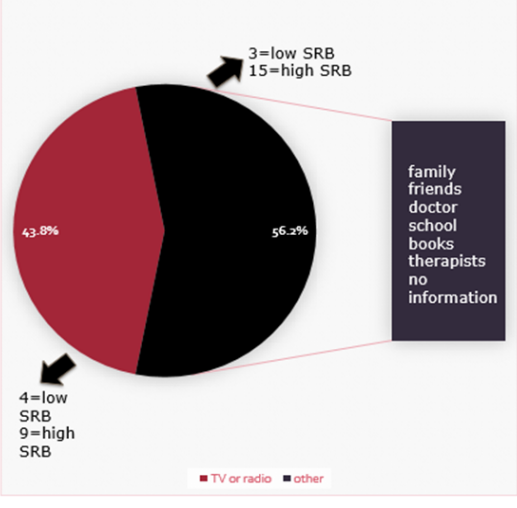

Figure 4. Relationship between Source of HIV/AIDS Information and SRB

A total of 158 coding references were made to artists/ celebrities, media, music, and religion. Fifteen references were made to artists/celebrities. Fifty-three references were made to media; Thirty-nine references were made to its negative influence and six to it having no influence. Forty-six references were made to music; five references were made specifically to hip hop. Forty-four references were made to religion (see Figure 5 and Table 1).

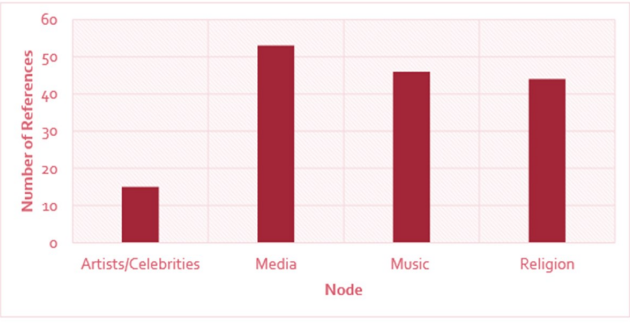

Figure 5. NVivo Coding References

Artists/Celebrities

When asked about the role of music, media, and internet in sexual decision making, the culture among AA adolescents, and how AA culture affects sexual decision making, references were made to a combination of artists and celebrities that the participants considered role models. One participant said, "they look up to the artists – and it's based on how they try to live their life, based on like – the popular rap artists like Wayne – and they get their dress and style from." Another participant said, "so you kind of want to I guess be like and be like, and just do stuff they do, 'cause you know that's what boys want or whatever" .

Media

When asked about the role of music, media, and internet in sexual decision making and how AA culture affects sexual decision making, references were made to a combination of music and the media. One participant said, "cause these movies, videos, songs – it – it don't have no limit, like they'll tell you anything – you can look at a video and you can see basically somebody having sex on the video…" .

Music

When asked to describe AA culture, the culture among AA adolescents, ways to express AA culture, and the influence of AA culture and social factors on AA adolescent females' sexual decision making, references were made to hip hop and music in general. One participant said, "I think that it's based mostly around hip hop and rap and they look up to the artists." When asked to describe the role of music, media, and the internet on sexual beliefs and behaviors, one participant said, "Well, as far as media, I think it has a big role on you especially when it has someone that's like – Lil Wayne for example, he's a big role model to a lot of boys and Nikki Minaj, I say for girls, and how they be all on the internet and TV and videos it affect a lot of youths…yeah, I say from 15 and under – they really don't understand, so I say it plays a big role on their sexual life." Another participant said, "it be the music we listen too. Cause now these days, you listen to a song and it is either talking about sex or it is talking about how to have sex" .

Religion

When asked to define culture in general, define AA culture, describe the values, beliefs, customs, and norms of AA culture, describe activities that are expressions of AA culture, and explain cultural and social factors that influence sexual beliefs and behaviors, 44 references were made to religiosity or spirituality. One participant said, "in our culture is, you know, going to church, putting God first, and to me, I think that is major because, growing up in a household where God came first, it's like, everything I do…"

Conclusions

AA adolescent females largely associate their culture, beliefs, and influential sexual factors with music, media, and religion. There was not a strong association in the transcripts between religiosity and sexual attitudes and behavior. Nonetheless, these findings help to highlight the role of these factors in AA adolescent girls' sexual beliefs and behaviors, as well as inform people who work with AA adolescent females so as to create more effective intervention programs.

Future Directions

Future directions include reviewing the interview transcripts and questionnaires a second time to find different factors more influential than music and religion in the sexual beliefs and behaviors of AA adolescent females. Possible variables for further analysis include familial influence and strength of cultural identity. After identifying factors with certainty, a tertiary analysis will then be conducted on these new factors using NVivo and SPSS software.

performances with feeding and fasting. Danny's future

plans are to work in veterinary medicine, possibly continuing his research in digestive physiology.

References

[1]Ball J, Armistead L, & Austin B. (2003). The relationship between religiosity and adjustment among African-American, female, urban adolescents. Journal of Adolescence, 431-446.

[2]Centers for Disease Control and Prevention. (2015). HIV Surveillance Report, 2014; vol. 26. Retrieved from: http://www.cdc.gov/hiv/library/reports/surveillance/.

[3]Cohen, M., Kahn, D., and Steeves, R. Hermeneutic phenomenological research. Sage Publications, Inc.

[4]Donenberg, G.R., Emerson, E., Bryant, F.B., Wilson, H., Weber-Shifrin, E. (2001). Understanding AIDS-risk behavior among adolescents in psychiatric care: Links to psychopathology and peer relationships. Journal of the American Academy of Child & Adolescent Psychiatry, 40, 642-5.

[5]Griffith DM, Campbell B, Allen JO, Robinson KJ, & Stewart SK. (2010). YOUR Blessed Health: An HIV-Prevention Program Bridging Faith and Public Health Communities. Public Health Reports, 4-11.

[6]Krueger, R., & M. Casey. (2000). Focus groups. Thousand Oaks, CA: Sage Publications, Inc.

[7]Martino SC, Collins RL, Elliott MN, Strachman A, Kanouse DE, & Berry SH. (2006). Exposure to Degrading Versus Nondegrading Music Lyrics and Sexual Behavior Among Youth. Pediatrics.

[8]McCree DH, Wingood GM, DiClemente R, & Harrington KF. (2003). Religiosity and Risky Sexual Behavior in African-American Adolescent Females. Journal of Adolescent Health, 2-8.

[9]Peterson SH, Wingood GM, DiClemente RJ, Harrington K, & Davies S. (2007). Images of Sexual Stereotypes in Rap Videos and the Health of African American Female Adolescents. Journal of Women's Health, 1157-1164.

[10]Primack BA, Douglas EL, Fine MJ, & Dalton MA. (2009). Exposure to Sexual Lyrics and Sexual Experience Among Urban Adolescents. American Journal of Preventive Medicine, 317-323.

[11] Rubin HS, & Rubin, IS. (2005). Qualitative interviewing: The art of hearing data. Thousand Oaks: Sage Publications.

[12]Ward LM, Hansbrough E, & Walker E. (2005). Contributions of Music Video Exposure to Black Adolescents' Gender and Sexual Schemas. Journal of Adolescent Research, 143-166.

Appendix

Node	References
Media	53
Negative Influence	39
No Influence	6
Music	46
Hip Hop	5

Table 1. Subcategories of Media and Music Coding References

Richard M. Myers, PhD
President, Science Director, & Faculty Investigator for Hudson Alpha Institute for Biotechnology

Dr. Myers, a world renown scientist, can trace his humble beginnings all the way back to the University of Alabama. In this new segment about successful UA science alumni JOSHUA spoke to Dr. Myers, who is the President of HudsonAlpha, about what inspired him to become a genomic scientist, his greatest achievements, his greatest setbacks, and his outlook on genetic research in the future.

Caitlin Thomas: It's best to start this conversation at the beginning, so what would you say interested you in your line of work?

Richard Myers: I'm a scientist who does research in human genetics, but I started out in college as a sociology major at the University of Alabama. Midway through I took a biology and chemistry course and ended up being offered a summer research job in a chemistry lab. I had no idea what it was going to be about; I thought the professor was crazy to offer a sociology major to work in his lab. As soon as I started doing research and learning the concepts of doing science and trying to discover and understand how the universe works I was hooked. I decided that's what I'm going to do.

I got into my current line of work, which I discovered as I was getting into my graduate and post-doctoral work, when I realized that we can start to think about how our genes contribute to what and who we are and I just got completely hooked on the idea of understanding that. That's what led me to studying human genetics and being a part of the Human Genome Project.

CT: You've published a lot of papers. It appears that you have your hands in a little of everything, form cancer research to Gulf War Syndrome. Have there been any surprising and/or interesting findings to you?

RM: Throughout my career there have always been surprises, which is really exciting. I can tell you some thing that is going on now that is not even published yet. One of my graduate students and later post-docs in the lab has collaborated with a friend and physician-scientist from Stanford to discover DNA markers that are almost 100% predictive of kidney cancer. Rarely do you get results that are that strong and this is such a strong test; it says will close to 100% accuracy, sensitive, and specificity that this tissue is kidney tumor tissue as opposed to normal tissue. The exciting thing about that is we're trying now to see if we can detect that, not by biopsy of the kidney but by finding in blood or urine the same DNA methylation marker. We were surprised that it was such a strong effect, rarely do you see biology being that compliant.

CT: Where do you feel your research is going in the future? What is your opinion on the current state of genomics and it's applicability to the common person?

RM: We are certainly already starting to practice genomic medicine using DNA and RNA information for deciding how much and which particular drug is appropriate for particular patients. We have a huge number of basic science discoveries left to make, but I think the fact that we've gone from sequencing one genome with two-thousand scientist in a 13 year period for 3 billion dollars, to now doing it for a few thousand dollars in a few days with relatively low hands-on is a huge, huge, huge, jump in our ability to gain knowledge and I think where we're heading is going to get even faster and cheaper to sequence whole genomes. We're heading where we could be practicing genomic medicine for everybody if we keep supporting research and making sensible decisions at a national level. Where we use the genome information to prevent disease. There's a huge opportunity to prevent disease by knowing what you're susceptible to and the interpretation of the genome will get better and better as we do more and more of that. There's 4 million babies born in the US a year and within a few years I think we will be sequencing every newborn. This isn't just about sequencing the genome, but using that information with all the other things as part of the preventative medicine side of medical care. It's an exciting time to be in this field because the increase in information is growing so rapidly and is just starting to be applied.

Caitlin Thomas is the Executive Editor of JOSHUA
This interview has been condensed and edited.

JOSHUA was made possible by the following organizations:

University of Alabama
Office of the President

Tri-Beta National Honor Society
Kappa Beta Chapter

Howard Hughes Medical Institute

National Science Foundation

Computer Based Honors Program

And by the 2015-2016 JOSHUA Editing Staff

2017 Submission Guidelines

We accept articles from current undergraduate students at The University of Alabama (UA). If you are a graduate student or recent alumnus of UA, we will consider your article if the majority of your work was conducted while you were an undergraduate at UA. Undergraduate students from other institutions may submit; however, priority will be given to those who conducted their research at UA.

1. Your name, e-mail address, and phone number must be included.

2. Your submission must relate to science or health.

3. Your work must be sponsored by a faculty member.

4. The length of your submission must be between 2000 and 4500 words. We will accept longer submissions if the author can limit the submission to the required length for the publication, and any extra material is able to be published online.

5. Figures, charts, and graphs are allowed but not required. (Note: The color will be mostly black and white.)

6. Your paper must contain an abstract.

7. Your citations must follow the guidelines listed on our website at BAMA.UA.EDU/~JOSHUA.

8. The deadline for submission is February 12, 2017.

9. E-mail submissions to joshua.alabama@gmail.com


SHELBY HALL

THE UNIVERSITY OF ALABAMA®